MOLECULAR MECHANISMS OF PI3K ISOFORM DEPENDENCE IN CARCINOGENESIS

A THESIS SUBMITTED TO
THE GRADUATE SCHOOL OF ENGINEERING AND SCIENCE
OF BILKENT UNIVERSITY
IN PARTIAL FULFILLMENT OF THE REQUIREMENTS FOR
THE DEGREE OF
MASTER OF SCIENCE
IN
MOLECULAR BIOLOGY AND GENETICS

By

Sena Atıcı

December 2020

MOLECULAR MECHANISMS OF PI3K ISOFORM DEPENDENCE IN CARCINOGENESIS

By Sena Atıcı

December, 2020

We certify that we have read this thesis and that in our opinion it is fully adequate, in scope and in quality, as a thesis for the degree of Master of Science.

Onur Çizmecioğlu
(Advisor)

Özlen Konu Karakayalı

Sreeparna Banerjee

Approved for the Graduate School of Engineering and Science:

Ezhan Karaşan
Director of the Graduate School of Engineering and Science

ABSTRACT

MOLECULAR MECHANISMS OF PI3K ISOFORM DEPENDENCE IN CARCINOGENESIS

Sena Atıcı
M.S. in Molecular Biology and Genetics
Advisor: Onur Çizmecioğlu
December, 2020

PI3K pathway is important for cellular proliferation, survival and metabolism. PTEN-loss and activating mutations of *PIK3CA* are most frequently seen PI3K related alterations in various cancer types. Activating mutations in *PIK3CA* could render tumors p110α dependent. Also, upon PTEN-loss, p110β isoform of ClassIA PI3Ks becomes prominent. Nevertheless, the mode of action of p110 prevalence is still not clear. Here, we aimed to understand the mechanism of the isoform dependence switch in PTEN-null cancer types. Firstly, we found that PTEN status had an impact on isoform prevalence in both MEFs and PC3s. p110α dependence decreased in PTEN-depleted MEFs and reciprocally there was a decrease in dependence to p110β in PTEN-reexpressed PC3 cells. On the other hand, upon modulation of PTEN expression, there was no complete switch-over in dependence from one ClassIA PI3K isoform to the other. Interestingly, when p110β overexpression was performed in PTEN depleted MEFs, cells became less dependent on p110α and more dependent on p110β for cellular viability. However, p110β overexpression in combination with PTEN status change did not again induce a complete isoform switch within ClassIA PI3Ks. To reveal additional modules involved in PI3K isoform prevalence, GSE21543 dataset was analyzed and mRNA levels of AK4, SQLE, CREB3L4 genes were found to be significantly upregulated in constitutively activated p110β in murine models of prostate cancer. Among these genes, SQLE,a rate limiting enzyme in cholesterol synthesis, is highly amplified in various tumor samples according to patient datasets. Breast and prostate cancers have relatively higher amplification rates of SQLE compared to other cancer types. The simultaneous incidence of PTEN mutation and SQLE amplification rate is also frequently observed in breast and prostate cancers. mRNA levels of cholesterol synthesis genes were upregulated in GSE21543 dataset

when the PI3K pathway was constitutively activated by p110β myristoylation. Also, the expression levels of the cholesterol synthesis genes were decreased upon PI3K repression with PTEN re-expression in our qPCR results. Constitutively activated p110β MEFs and PTEN-null prostate, breast cancer cell lines were found to be sensitive to inhibitors of rate-limiting enzymes of cholesterol synthesis pathway. Besides in-line with mRNA levels, SQLE protein levels were decreased in PTEN re-expressed prostate cancer cell lines. On the other hand, SQLE protein levels were stabilized upon PTEN expression with protease inhibitor treatment which indicates that PTEN and PI3K activity may affect SQLE transcriptionally as well as post-translationally. We also demonstrated that tamoxifen therapy responders have lower survival rate and higher SQLE expression according to patient data. In line with this data, in cellular models of tamoxifen resistant breast cancer, we have seen elevated levels of SQLE. All in all, our data emphasizes the critical importance of cholesterol synthesis pathway as a metabolic effector of the PI3K pathway and we can speculate that p110β dependence in PTEN-null cancer types might arise as a result of its excessive activation.

Keyword: PTEN-null, PI3K, terbinafine, cholesterol synthesis, SQLE

ÖZET

Karsinojenezde PI3K İzoform Bağımlılığı Değişikliğinin Moleküler Mekanizması

Sena Atıcı

Moleküler Biyoloji ve Genetik, Yüksek Lisans

Tez danışmanı: Onur Çizmecioğlu

Aralık, 2020

PI3K hücresel büyüme ve hücre sağkalımı açısından önemli bir yolaktır. Kanser hücrelerinde, PTEN kaybı ve *PIK3CA* gen mutasyonu fazlaca görülen PI3K mutasyonlarındandır. *PIK3CA*'daki geninde olan aktive edici mutasyonlar, tümörleri p110α'ya bağımlı hale getirir. Ayrıca, PTEN yetersizliğinde, p110β izoformu baskın SınıfIA üyesi haline gelir. Bununla birlikte, p110 prevalansı için mekanizmalar tam olarak açığa çıkmadı ve araştırmamızda, PTEN yetersiz kanser türlerinde isoform bağımlılığı değişikliğinin altında yatan mekanizmayı anlamayı amaçladık. İlk olarak, PTEN ekspresyon seviyesindeki değişimlerinin hem MEF'lerde hem de PC3'lerde baskın izoform bağımlılığında bir azalmaya neden olduğunu bulduk. Dolayısıyla, PTEN nakavtı yapılan MEF'lerde p110α bağımlılığı azaldı ve PTEN ifade edilen PC3'lerde p110β'ya bağımlılıkta bir azalma oldu. Bunun yanı sıra, PTEN ekspresyon seviyesi değiştiğinde, baskın olmayan diğer SınıfIA PI3K izoformlarına bağımlılıkta herhangi bir değişiklik olmadı. Daha sonra, PTEN nakavtı yapılan MEF'lerde yapısal etkin p110β ekspresyonu gerçekleştirildiğinde, hücreler p110a'ya daha az bağımlı hale geldi ve hücresel canlılık için p110β izoformlarına daha fazla bağımlı hale geldi. Bununla birlikte, hem konstitütif olarak aktifleştirilmiş p110β ifadesi hem de PTEN ekspresyon değişikliği SınıfIA PI3K'leri için tam olarak izoform değişimi sağlayamadı. PI3K izoform prevalansında yer alan ilave modülleri ortaya çıkarmak için, GSE21543 veri seti analiz edildi ve *AK4, SQLE, CREB3L4* genlerinin, konstitütif olarak aktifleştirilmiş p110β içeren murin prostat kanseri modellerinde önemli ölçüde yukarı regüle edildiği bulundu. Ayrıca, hız belirleyici bir kolesterol sentez enzimi olan SQLE, hasta verilerindeki çeşitli tümör örneklerinde yüksek oranda amplifiye edilmiştir. Meme ve prostat kanserleri diğer kanserlere göre nispeten daha yüksek amplifikasyon oranlarına sahiptir, PTEN mutasyonu ve SQLE amplifikasyon oranının aynı anda görülme oranı da meme ve prostat kanserlerinde daha yüksektir. PI3K yolağı

p110β miristilasyonuyla yapısal olarak aktive edildiğinde, GSE21543 veri setinde kolesterol sentez genlerinin mRNA seviyeleri yukarı regüle edildi. Ayrıca, qPCR sonuçlarımızda PTEN'in yeniden ekspresyonu ile PI3K baskılanması SQLE mRNA seviyelerini azalttı. Yapısal olarak aktive edilmiş p110β içeren MEF'ler ve PTEN-yetersiz prostat ve göğüs kanseri hücre hatları, kolesterol sentez yolunun hız sınırlayıcı enzimlerinin inhibitörlerine sansitiftir. mRNA seviyelerinin yanı sıra, SQLE protein seviyeleri, PTEN yeniden eksprese edilen prostat kanseri hücre hatlarında azaldı. Diğer yandan PTEN eksprese edilmiş prostat kanser hatlarında, SQLE seviyeleri, proteaz inhibitörü uygulanması ile stabilize edildi. Bu PTEN ve PI3K aktivitesinin, SQLE transkripsiyonunun yanı sıra translasyon sonrası olarak etkileyebileceğini göstermektedir. Ayrıca tamoksifen tedavisine yanıt verenlerin, hasta verilerine göre daha düşük hayatta kalma oranına ve daha yüksek SQLE ekspresyonuna sahip olduğunu da gösterdik. Bu veriler doğrultusunda, tamoksifen dirençli meme kanserinin hücresel modellerinde, yüksek SQLE seviyeleri gördük. Sonuç olarak, verilerimiz kolesterol sentez yolunun PI3K yolağının bir metabolik efektörü olarak kritik önemini vurgulamaktadır ve PTEN-null kanser türlerinde p110β bağımlılığının aşırı aktivasyonunun bir sonucu olarak ortaya çıkabileceğini tahmin edebiliriz.

Anahtar kelimeler: PTEN-noksanlığı, PI3K, terbinafine, kolesterol sentezi, SQLE

To my parents…
Sevgili Aileme…

Acknowledgements

I would like to thank my advisor Assist. Prof. Dr. Onur Çizmecioğlu for his supports and valuable supervision during my Master's studies. Also, I would like to express my gratitude to him for always being so kind, thoughtful and his valuable mentoring.

I would like to thank my colleagues at OC lab group and Bilkent MBG family for their helps and valuable friendships during my Master's period.

Also, I would like to express my thanks to Assist. Prof. Dr. Nihal Terzi Çizmecioğlu and her laboratory members for helping me about qPCR experiments.

Additionally, I would like to thank Assoc. Prof. Özgür Şahin and his laboratory members for giving tamoxifen resistant breast cancer lines and their helps.

I would like to thank my friends, Gizem Tuğçe Ulu and Aydoğa Kallem for valuable friendship and being always there for me to share my happiness, anger, sadness. Also, I would also like to thank my cousin Aydoğa Kallem for opening her house for me and being like my sister during this difficult corona period and my life.

At last but not least, I would like to express my gratitude and respect to my mother Ayten Atıcı and my father Mehmet Siyami Atıcı who were so supportive, patient and they were best parents. I am the luckiest person to have them in my life.

This project is supported by Tübitak grant project number 118Z976.

Teşekkürler

Danışmanım Yrd. Doç. Dr. Onur Çizmecioğlu'na yüksek lisans eğitimim sırasında destekleri ve değerli danışmanlığı için teşekkür ederim. Ayrıca her zaman bu kadar nazik ve düşünceli olduğu için ve değerli danışmanlığı için kendisine teşekkürlerimi sunuyorum.

Yüksek Lisans dönemim boyunca yardımları ve değerli dostlukları için OC laboratuvar grubundaki meslektaşlarıma ve Bilkent MBG ailesine teşekkür ederim.

Ayrıca Yrd. Doç. Dr. Nihal Terzi Çizmecioğlu'na ve laboratuar üyelerine qPCR deneylerinde yardımcı oldukları için teşekkürlerimi sunuyorum.

Ayrıca tamoksifen dirençli meme kanseri hatlarını verdikleri ve yardımları için Prof. Özgür Şahin ve laboratuvar üyelerine teşekkür ederim.

Arkadaşlarım Gizem Tuğçe Ulu ve Aydoğa Kallem'e değerli dostlukları ve mutluluk, öfke, üzüntülerimi paylaşmam için hep yanımda oldukları için teşekkür ederim. Ayrıca kuzenim Aydoğa Kallem'e bu zorlu korona döneminde bana evini açtığı ve hayatım boyunca kardeşim gibi olduğu için çok teşekkür ederim.

Ve son olarak, çok destekleyici, sabırlı ve en iyi anne-baba olan annem Ayten Atıcı ve babam Mehmet Siyami Atıcı'ya şükran ve saygılarımı sunuyorum. Hayatımda oldukları için dünyanın en şanslı insanıyım.
Bu proje Tübitak 118Z976 projesi tarafından desteklenmiştir.

Table of Contents

List of Figures

List of Tables

Abbreviations

AdCre Adenovirus Expressing Cre Recombinase

AKT AKT Serine/Threonine Kinase

AK4 Adenylate Kinase 4

AR Androgen Receptor

BH BCR Homology

CE Cholestryl Ester

CREB3L4 Cyclic Amp Responsive Element Binding Protein Like 4

DTT Dithiothreitol

FDPS Farnesyl Diphosphate Synthase

FOXO Forkhead Box Protein O

FPP Farnesyl Pyrophosphate

GPCR G-Protein Coupled Receptors

GPP Geranylgeranyl Pyrophosphate

GSK3β Glycogen Synthase Kinase 3

HMGCS 3-Hydroxy-3-Methylglutaryl-CoA Synthase

HMGCR 3-Hydroxy-3-Methylglutaryl-CoA Reductase

MEF Mouse Embryonic Fibroblast

mTOR Mammalian Target of Rapamycin

MVD Mevalonate-5-pyrophosphate Decarboxylase

MVK Mevalonate Kinase

PCa Prostate Cancer

PDK1 Phosphoinositide-dependent Kinase 1

PH Pleckstrin Homology

PHTS PTEN Hamartoma Syndromes

PKB Protein Kinase B

PI Phosphadylinositol

PI3K Phosphoinositide 3-kinase

PI-4-P Phosphadylinositol-4-phosphate

PI-3,4-P2 Phosphadylinositol-3,4-bisphosphate

PI-4,5-P2 Phosphatidylinositol-4,5-bisphosphate

PIP3 Phosphatidylinositol-3,4,5-trisphosphate

PtdIns Phosphatidylinositol

PMVK Phosphomevalonate Kinase

PTEN Phosphatase and Tensin Homolog

PX Phox Homology

RBD Ras Binding Domain

RTK Receptor Tyrosine Kinase

SDS Sodium Dodecyl Sulfate

SH2 Src-homology 2

SH3 Src-homology 3

SREBP Sterol regulatory element-binding protein

SQLE Squalene Epoxidase

TSC2 Tuberous Sclerosis Complex 2

qRT-PCR Quantitative Real Time Polymerase Chain Reaction

Chapter 1

1 Introduction

1.1 PI3K pathway

Phosphoinositide 3-kinase (PI3K) pathway mainly involves in proliferation, growth, survival and cellular metabolism (Figure 1.1). PI3Ks has lipid kinase activity and phosphorylate phosphatidylinositol (PtdIns) lipids at 3'-hydroxyl group (D3 position)[1]. Phosphorylated phosphatidylinositol molecules play role as a secondary messenger in cells and cause activation of Akt which is a serine threonine kinase and other downstream molecules. The main suppressor of the PI3K is phosphatase tensin homolog (PTEN) [2].

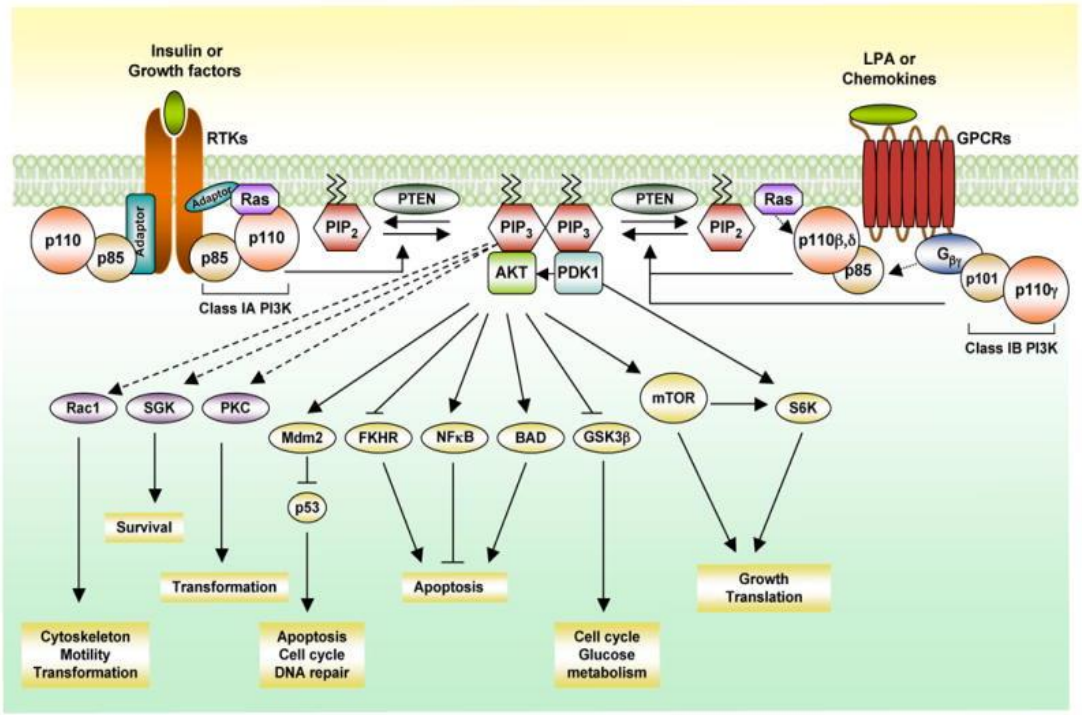

Figure 1.1: PI3K pathway components. PI3K pathway activated via RTKs and GPCRs and downstream components were activated [2].

PI3Ks are classified into 3 groups according to their functions and structures. Class I PI3Ks produce phosphatidylinositol-3,4,5-trisphosphate (PIP3) from phosphatidylinositol-4,5-bisphosphate (PI-4,5-P2) phosphorylation. Class II PI3Ks

phosphorylate both phosphadylinositol-4-phosphate (PI-4-P), phosphadylinositol (PI) to produce phosphadylinositol-3,4-bisphosphate (PI-3,4-P2), phosphadylinositol-3-phosphate (PI-3-P), respectively. Class III PI3Ks produce only PI-3-P molecules from PI [1]. PI3Ks are activated via various growth factors and cytokines through the receptor tyrosine kinases (RTK) and G-protein coupled receptors (GPCR). PI3Ks contain a heterodimeric structure formation that is composed of the catalytic subunit and regulatory subunit [3].

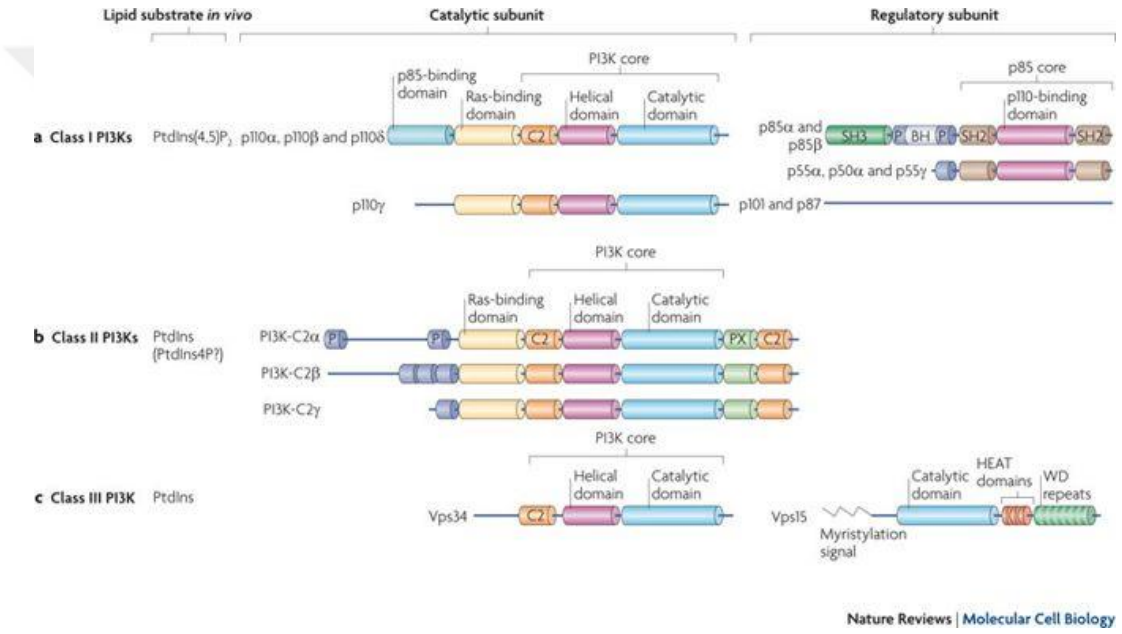

Figure 1.2: Domain structures of PI3Ks' catalytic and regulatory subunits. PI3Ks divided into 3 main classes. **a)** ClassI PI3Ks consists of p110α, p110β, p110δ, p110γ isoforms. **b)** ClassII PI3Ks consists of PI3K-C2α, PI3K-C2 β, PI3K-C2γ. **c)** Vps34 isoform exists in the ClassIII PI3Ks **[4].**

1.1.1 ClassI PI3Ks

ClassI PI3Ks are separated into 2 groups according to regulatory subunit types; ClassIA isoforms form heterodimers with p85 molecules and ClassIB heterodimerize with p101 regulatory subunits [3]. Regulatory subunits of ClassIA PI3Ks are *PIK3R1* (p85α), *PIK3R2* (p85β), *PIK3R3* (p55γ) genes. p55α and p50α versions of regulatory

subunits are produced from *PIK3R1* gene with splicing mechanism. Regulatory subunits mainly have binding domain for p110s (inter SH2 domain) and 2 SH2 (Src-homology 2) domains that exist at N-terminal and C-terminal. Longer isoforms of regulatory subunits like p85α and p85β have additional SH3 (Src-homology 3) and BH (BCR homology) domains. SH2 domain of p85s mediate recruitment of p110s to the phospho-tyrosine residues as YXXM motifs of receptors for activation [5, 6]. Different molecules bind to lipids through their pleckstrin-homology (PH), phox homology (PX) and FYVE domains.

ClassIA PI3Ks contains three p110 isoforms; p110α encoded by *PIK3CA* gene, p110β encoded by *PIK3CB* gene and p110δ encoded by *PIK3CD* gene. ClassIB consists of p110γ that is coded by *PIK3CG* gene (Figure 1.2). ClassI PI3Ks share similar structures, but they have different functions in cells. p110α and p110β isoforms expressed ubiquitously in many tissues, but p110γ and p110δ isoforms mainly expressed in hematopoietic cells [3, 7]. Besides the regulatory subunits, small GTPases bind to PI3Ks via the RAS-binding domain (RBD) for activation. Ras family proteins activate p110α, p110γ PI3K isoforms. Rho GTPase family proteins which are RAC, Cdc42 activate p110β isoform [8, 9]. Activation of PI3Ks leads to phosphorylation of PIP2 molecules into PIP3 and PH domain containing proteins were recruited to plasma membrane where PI3K activation occurs. Mostly studied PI3K pathway downstream molecule which has PH domain is Akt (protein kinase B(PKB)) and undergo conformational change after binding to PIP3 molecules. Akt is phosphorylated via phosphoinositide-dependent kinase 1 (PDK1) and phosphorylation of Akt leads activation and phosphorylates many molecules like glycogen synthase kinase 3 (GSK3β), forkhead box protein O (FOXO) [10]. Beside of the Akt, SGK3 is activated via PDK1 activity and activate downstream molecules in Akt-independent path. However, Akt and SGK3 share some target molecules beside of their unique targets [11, 12].

1.1.2 PTEN

PTEN (Phosphatase and Tensin Homolog) is a haploinsufficient tumor suppressor as its decreased expression accompanies cancer progression with increased tumor size and worse prognosis in patients [13]. PTEN mutations and homozygous deletions are seen mostly in cancer types like glioblastoma, prostate cancer, breast cancer. PTEN mutations become significantly higher in advanced stages. So, it is suggested that it is involved in progress of cancer rather than initiation of cancer progress [14]. Also, germline PTEN mutations increase risk of cancer-like syndromes such as PTEN hamartoma syndromes (PHTS), Proteus syndrome, Cowden syndrome [15].

PTEN has dual phosphatase activity that dephosphorylate both lipids and proteins. As a lipid phosphatase, its function provides conversion of PtdIns(3,4,5)P_3 into PIP2 and prevent activation of downstream components of PI3K pathway [16]. Besides the mutations and inactivation of PTEN allele, compartmentalization of PTEN proteins are important for cancer progress. PTEN post-translational modifications as acetylation, oxidation, phosphorylation play role in compartmentalization.

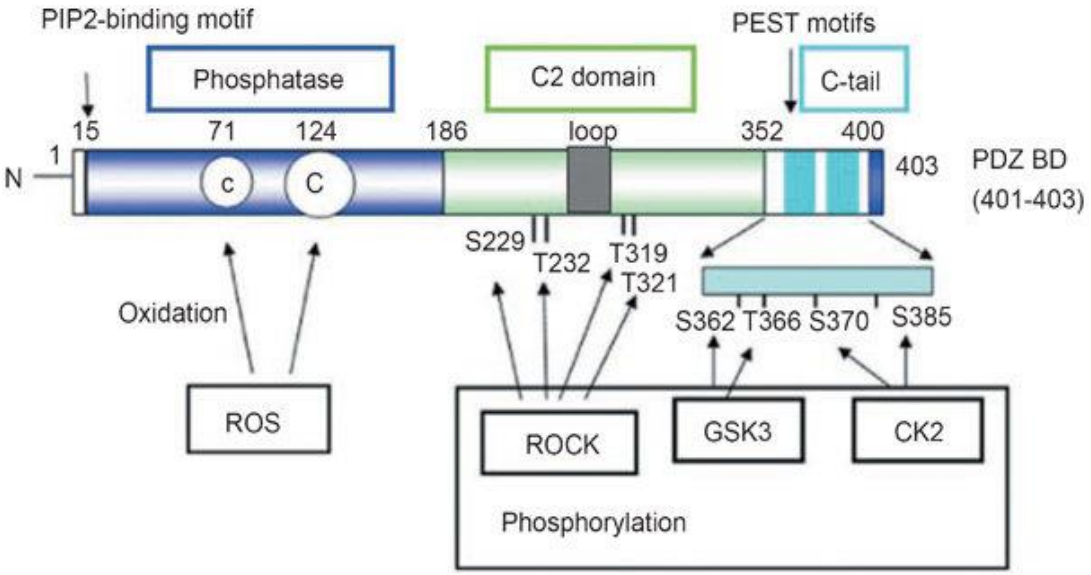

Figure 1.3: Domain structure of PTEN. PTEN has PBD (PIP2 binding motif), phosphatase, C2, C-terminal tail, PDZ BD (PDZ domain-binding motif) domains [17].

PTEN consists of 5 main domains (Figure 2). C2 domain provides lipid or membrane binding of the molecule, C-terminal tail contains PEST (Pro, Glu, Ser, Thr) motifs [17]. With PDZ BD motif PTEN dephosphorylate proteins at Ser, Thr, Tyr residues [18].

p53, PI3K, Hippo, Myc, RTK Ras pathways were examples of highly mutated pathways in different cancer types. Among the PI3K pathway components' most of alterations exist as *PIK3CA* activating mutations, *PTEN* deletion or loss of function, *AKT* amplification or gain of function mutations, amplification of RTKs that is required for PI3K activation [19, 20]. According to TCGA database that contains 9125 samples from 33 different cancer types, RTK-Ras pathway has the highest alteration frequency in cancer types at 46% [21]. Next generation sequencing data from 19784 tumors demonstrated that, 38% of patients have at least one type of PI3K related aberration. 13% of samples have *PIK3CA* mutation, 30% have *PTEN*-loss, 6% have *PTEN*-mutations, 1% have *AKT1*-mutations [22].

1.1.3 Regulation of Cellular Metabolism by PI3K Pathway

PI3K pathway activation is provided by many growth factor molecules' through their receptors. In response to these growth factors, PI3K pathway plays roles in many metabolic processes such as glucose and lipid metabolism, nucleotide synthesis by direct phosphorylation or transcriptional regulation. Several molecules like mTOR, FOXO, GSK3 were phosphorylated by Akt that is downstream of PI3Ks [23]. mTOR pathway orchestrate homeostasis between hormone, growth signaling and anabolic, catabolic reactions [24].

1.2 Cholesterol Biosynthesis Pathway

Cholesterol is an important lipid molecule and building block of the steroids. Cholesterol is required for membrane structure and it is especially enriched in lipid rafts. Cholesterol synthesis begins with production of mevalonate from acetate. HMGCR catalyze reduction of HMG-CoA into mevalonate. Mevalonate is converted into farnesyl pyrophosphate (FPP) with several steps and FPP, GGPP (geranylgeranyl

pyrophosphate) molecules are required for prenylation. Prenylation is a type post-translational modification occurring on proteins like Ras, Rho GTPases. Prenylation anchors modified proteins to the cell membrane and provide protein localization in cells [25, 26]. Squalene epoxidase (SQLE) gene catalyze formation of 2,3-epoxysqualene from Squalene. *HMGCR* and *SQLE* genes are rate-limiting enzymes at cholesterol pathway **(Figure 1.4).**

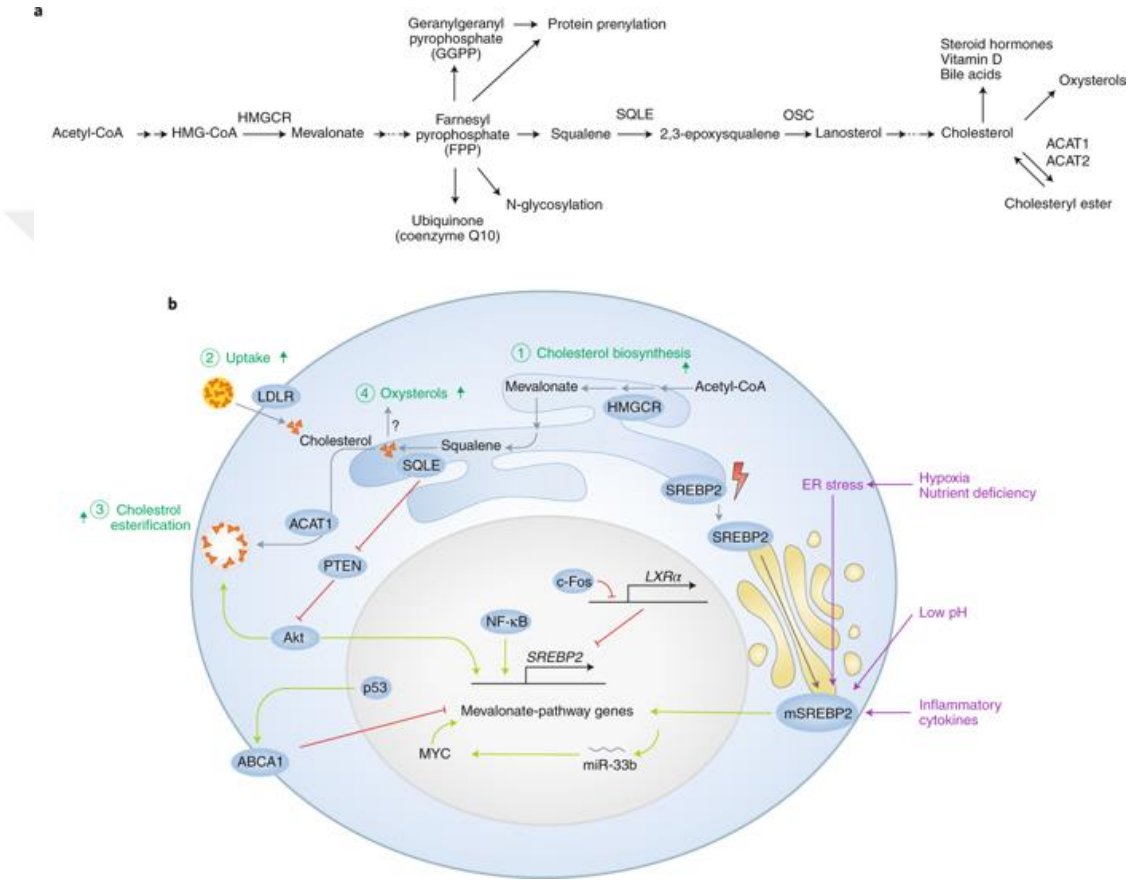

Figure 1.4: Cholesterol biosynthesis pathway. a) Cholesterol is produced from acetyl-CoA and enzymes that involves in the cholesterol synthesis. **b)** Cholesterol pathway relation with PI3K pathway [27].

1.3 Cholesterol – Cancer Relation

Cholesterol expression and related enzyme activities are strictly regulated and cholesterol pathway enzymes are mainly controlled by SREBP transcription factors. Sterol regulatory element-binding protein (SREBP) gene was upregulated in some cancer types like glioblastoma, prostate [28]. The need for cholesterol becomes higher

in cancer cells for membrane and other functions. High cholesterol levels in blood increase the prostate cancer (PCa) progression rate. To increase cholesterol levels, cells transport cholesterol with ABCA1. However, in cancer cells, ABCA1 level is decreased and cells begin to synthesize cholesterol *de novo* [29]. With the *de novo* cholesterol synthesis, SQLE expression levels increase in high grade prostate cancer cells and PCa cells produce cholesterol at a high rate instead of uptake of cholesterol from blood stream. Also, this notion coincided with decreased level of LDLR in aggressive PCa cells [30]. Cholestryl ester (CE) molecules are stored via lipid droplets. CE accumulated in metastatic PCa cells compared to the other stages of cancer or prostate tissue. PTEN-loss and PI3K-mTOR pathway upregulation cause increase in CE accumulation [31].

Prostate cells' proliferation and development of prostate cancer mainly depends on steroid hormone - androgen. For treatment of PCa, prostatectomy, radiation, hormone therapy (androgen deprivation therapy) are common ways. Some androgen-dependent cancers undergo regression but many patients recur androgen-independent PCa upon androgen deprivation therapy. Mutations of androgen receptor occur mainly during the metastatic stage of PCa at higher rates compared to early stages [32]. Recurring cells survive via alternative pathways like PI3K, MAPK and cells become sensitive to low androgen concentration with higher androgen-receptor expression [33, 34]. PTEN loss is mostly seen during metastatic PCa cells and causes over-activation of PI3K pathway. According to *in vitro* and *in vivo* studies, conditional PTEN-loss converts androgen dependence into androgen-independent growth [35]. Because of the reciprocal relation between PI3K pathway and ARs, some treatment options contain combinational drug treatments of PI3K or mTOR inhibitors with combination of AR inhibitors [36, 37].

Cholesterol-lowering agents are used for cancer treatments taking advantage of high need of cholesterol in cancer cells. Statins are widely known cholesterol-lowering agents and target HMGCR enzyme that is the first rate limiting enzyme of cholesterol biosynthesis. Statins are used for prostate, breast, head and neck cancer treatments as mono or combinational therapy [38-40].

1.4 Aim of the Study

PI3K pathway is important for cellular proliferation, metabolism. PI3K pathway components' mutations were mostly seen mutation types in various cancer cells. PTEN loss was one of the common aberrations in cancer types like prostate cancer, breast cancer, glioblastoma. Upon PTEN-loss, cancer cells become more dependent on p110β for cellular proliferation. In this study, we tried to understand the signaling components that lead to isoform dependence change in PI3K and cholesterol pathway's role in the PTEN-null cancers. In order to tackle this problem, I generated PTEN-loss and PTEN-reexpressed cellular models. Besides, we aimed to see relation of cholesterol synthesis pathway enzymes with PI3K upon pathway activation or repression by PTEN. For this relation, cholesterol pathway related inhibitors – statin and terbinafine were used in PTEN-loss models of breast and prostate cancers.

Aims of the study can be listed as,

- Understanding molecular mechanisms of ClasIA isoform prevalence in cellular models of cancer
- To explore the relation of cholesterol synthesis genes with PI3K pathway
- To understand biomarker potential of SQLE in cancer

Chapter 2

2 Materials and Methods

2.1 Materials

2.1.1 Buffers

Table 2.20: Western blotting solutions and ingredients

Solutions	Ingredients
1X Cell Lysis Buffer	1X RIPA 1X Phosphatase inhibitor mix 1X Protease inhibitor 0.1μM DTT 1mM Na_3VO_4
10X transfer buffer	250mM Trizma-base 2M Glycine
10X TBS (pH = 7.4)	80 g NaCl 2 g KCl 250mM Trizma-base
10X Running Buffer	250mM Trisma-base 2M glycine 10g SDS
50X TAE	2M Trisma-base 57.1 mL acetic acid 10% (v/v) 0.5M EDTA
Stacking Gel Buffer (pH=6.8)	0.5M Tris-base pH adjusted to 6.8 with HCl
Resolving Gel Buffer (pH=8.8)	1.5M Tris-base pH adjusted to 8.8 with HCl

Table 2.21: Proliferation assay buffer solution ingredients

Solutions	Ingredients
Fixation Solution	10% acetic acid (v/v) 10% ethanol (v/v)
Destaining Solution	10% acetic acid (v/v)
Crystal Violet Stain	0.4% crystal violet stain (v/v) 20% ethanol (v/v)

2.1.2 Chemicals and reagents

Table 2.22: Cloning reagents and vectors

Catalog #	Compound Name	Brand
M0202S	T4 DNA Ligase	New England Biolabs, US
	10X T4 DNA Ligase Buffer	New England Biolabs, US
47916	pRXTN retroviral vector	Addgene, US
10785	pBabe-puroL-PTEN retroviral vector	Addgene, US
R3101S	EcoRI-High Fidelity Restriction Enzyme	New England Biolabs, US
R3136S	BamHI-High Fidelity Restriction Enzyme	New England Biolabs, US
C3040I	NEB Stable Competent *E. coli* (High Efficiency)	New England Biolabs, US
N3232L	1kb DNA ladder	New England Biolabs, US
48501.01	LB Medium	Serva, Germany
M0371L	Shrimp Alkaline Phosphatase (rSAP)	New England Biolabs, US
10835269001	Ampicillin	Roche, US

2.1.3 Cell culture media and components

Table 2.23: Cell culture media and materials that used in cell culture

Catalog #	Compound Name	Brand
D6429-500mL	DMEM – Dulbecco's Modified Eagle's Medium – High Glucose	Sigma-Aldrich, US
41966-029	DMEM (1X) Dulbecco's Modified Eagle's Medium	Gibco, US
52400-025	RPMI 1640 Roswell Park Memorial Institute 1640 Medium	Gibco, US
S1810-500	Fetal Bovine Serum	Biowest, US
S181T-500	Fetal Bovine Serum Tetracycline Free	Biowest, US

M7145-100mL	MEM Non-essential Amino Acid Solution (100x)	Sigma-Aldrich, US
15140-122	Penicillin - Streptomycin	Gibco, US
25300-054	Trypsin-EDTA (0,05%)	Gibco, US
L3000-008	Lipofectamine 3000 Transfection Reagent	Thermo Scientific, US
11668-027	Lipofectamine 2000 Transfection Reagent	Thermo Scientific, US
S1792	Simvastatin	Selleckchem, US
S2814	Alpelisib (BYL719)	Selleckchem, US
S1462	AZD6482 (KIN193)	Selleckchem, US
S2226	Idelalisib (Cal101)	Selleckchem, US
10011619	Terbinafine (hydrochloride)	Cayman Chemical, US
AB-101L	Nourseothricin - Solution	Jena Bioscience, Germany
D9891-1G	Doxycycline Hyclate	Sigma-Aldrich, US
10131-035	Geneticin (G418 Sulfate)	Gibco, US
A11138-03	Puromycin	Gibco, US

Table 2.24: Cell culture consumables

Catalog #	Compund Name	Brand
628160	Cell Culture dish, 100/20 mm	Greiner bio-one, Germany
665180	Cell Culture dish, 100/20 mm	Greiner bio-one, Germany
606180	Pipette, 5 ML	Greiner bio-one, Germany
607180	Pipette, 10 ML	Greiner bio-one, Germany
760180	Pipette, 25 ML	Greiner bio-one, Germany
771290	Micro-Pipette Tip, 0.5-10µL	Greiner bio-one, Germany
739290	Pipette Tips, 10 – 200 µL	Greiner bio-one, Germany
657160	Cell Culture Multiwell Plate, 6 Well	Greiner bio-one, Germany
665180	Cell Culture Multiwell Plate, 12 Well	Greiner bio-one, Germany

Table 2.25: Western blotting materials

Catalog #	Compound	Brand Name

161-0747	4x Laemmli Sample Buffer	Bio-Rad, US
10688.01	Acrylamide/Bis Solution, 37.5:1 (30w/v)	Serva, Germany
RPN2209	Amersham ECL Western Blotting Detection Reagent	Amersham Life Science, UK
34075	SuperSignal West Dura Extended Duration Substrate	Thermo Scientific, US
11930.03	Albumin Bovine Fraction V, pH 7.0	Serva, Germany
BR 1610393	Precision Plus Protein All Blue Protein Ladder	Bio-Rad, US
23391.02	Glycine	Serva, Germany
39055.01	Phosphatase Inhibitor Mix	Serva, Germany
P0758S	Sodium Orthovanadate (Vanadate)	New England Biolabs, US

Table 2.26: Primary and secondary antibodies

Catalog #	**Compound**	**Brand Name**
2118S	GAPDH (14C10) Rabbit mAb	Cell Signaling Technology, US
40659S	SQLE Antibody	Cell Signaling Technology, US
42201S	HMGCS1 (D1Q9D) Rabbit mAb	Cell Signaling Technology, US
9559S	PTEN (138G6) Rabbit mAb	Cell Signaling Technology, US
9272S	Akt Rabbit Ab	Cell Signaling Technology, US
9018P	Phospho-Akt1 (Ser473) (D7F10) XP Rabbit mAb (Akt1 specific)	Cell Signaling Technology, US
4056S	Phospho-Akt (Thr308) (244F9) Rabbit mAb	Cell Signaling Technology, US
9234S	Phospho-p70 S6 Kinase (Thr389) (108D2) Rabbit mAb	Cell Signaling Technology, US
2317S	S6 Ribosomal Protein (54D2) Mouse mAb	Cell Signaling Technology, US

2215s	Phospho-S6 Ribosomal Protein (Ser240/244)	Cell Signaling Technology, US
4858S	Phospho-S6 Ribosomal Protein (Ser235/236) Rabbit mAb	Cell Signaling Technology, US
7076S	Anti-Mouse IgG, HRP-Linked	Cell Signaling Technology, US
7074S	Anti-Rabbit IgG, HRP-Linked	Cell Signaling Technology, US

Table 2.27: Kits

Catalog #	Compound Name	Brand
10009365	MTT Cell Proliferation Assay Kit	Cayman Chemical, US
23225	Pierce BCA Protein Assay	Thermo Scientific, US
D2500-01	E.Z.N.A Gel Extraction Kit	Omega Bio-tek, US
D6492-01	E.Z.N.A Cycle Pure Kit	Omega Bio-tek, US
D6904-03	E.Z.N.A Plasmid Midi Kit	Omega Bio-tek, US

Table 2.28: qPCR components

Catalog #	Compound Name	Brand
15596026	Trizol Reagent	Invitrogen, US
74134	Rneasy Plus Mini Kit	Qiagen, Germany
170-8891	iScript cDNA Synthesis Kit	Bio-Rad, US
BR HSP9601	Hard-Shell 96-Well PCR Plates Sybr-green	Bio-Rad, US

Table 2.29: qPCR primer sequences

Primer Name – Gene	Primer Sequence
Human-HMGCS-forward	GGGCAGGGCATTATTAGGCTAT
Human-HMGCS-reverse	TTAGGTTGTCAGCCTCTATGTTGAA
Human-HMGCR-forward	GGACCCCTTTGCTTAGATGAAA
Human-HMGCR-reverse	CCACCAAGACCTATTGCTCTG

Human-FDPS-forward	CTTCCTATAGCTGCAGCCATGTAC
Human-FDPS-reverse	GCATTGGCGTGCTCCTTCT
Human-MVD-forward	TGAACTCCGCGTGCTCATC
Human-MVD-reverse	CGGTACTGCCTGTCAGCTTCT
Human-PMVK-forward	CCGCGTGTCTCACCCTTT
Human-PMVK-reverse	GACCGTGCCCTCAGCTCAT
Human-MVK-forward	TGGACCTCAGCTTACCCAACA
Human-MVK-reverse	GACTGAAGCCTGGCCACATC
Mouse-HMGCS-forward	TTTGACCGAGGGCTCCGTGG
Mouse-HMGCS-reverse	TCCAGGGCGCTGAGGTAGCA
Mouse-HMGCR-forward	TGTGGGAACGGTGACACTTA
Mouse-HMGCR-reverse	CTTCAAATTTTGGGCACTCA
Mouse-FDPS-forward	TCGGGTGAAAGCACTGTATG
Mouse-FDPS-reverse	GCACTGCTCTATGAGACTCTTG
Mouse-MVD-forward	TAGTCCACCGCTTCAACACC
Mouse-MVD-reverse	CCGACCTGAGTGGCAATGAT
Mouse-PMVK-forward	TTGCTTCTACTGAGCGGGTC
Mouse-PMVK-reverse	TTGTAGGTGCTCGCATCCAG
Mouse-MVK-forward	CGGGGCAGAAGTCTCAGAAG
Mouse-MVK-reverse	TGGGTACCGAGACATCACCT

Table 2.30: shRNA constructs

Construct Name	**Sequence**
pLKO.1-puro mouse shPTEN1	CCGGGCTAGAACTTATCAAACCCTTCTCGAGAAG GGTTTGATAAGTTCTAGCTTTTT
pLKO.1-puro mouse shPTEN2	CCGGCGACTTAGACTTGACCTATATCTCGAGATAT AGGTCAAGTCTAAGTCGTTTTTG

Table 2.31: Equipments

Mini-Protean Tetra Cell	Bio-Rad, US
Amersham Imager 600	GE Healthcare, US
Centrifuges	Hettich, Germany
	Nuve, Turkey
Cell Culture Hood	Nuaire, US
CO_2 Incubator	Thermo Scientific, US
Nanodrop One	Thermo Scientific, US
Synergy HT Microplate Reader	Biotek, US

2.2 Methods

2.2.1 Doxycycline inducible vector construction

pBabe-puroL-PTEN-wt, pBabe-puroL-PTEN-C124S and pRXTN overexpression vectors were double digested with EcoRI-HF and BamHI-HF enzymes. Reaction was prepared according to **Table 13** and incubated at 37ºC for 2 hours. Digested pBabe-puroL-PTEN vector was run on the gel, the band for PTEN (1200bp) was cut from the gel and gel purification was done with EZNA gel extraction kit according to manufacturer's protocol. Digested pRXTN vector was purified with EZNA cycle pure kit according to manufacturer's protocol. Concentrations were measured with Nanodrop.

Table 2.32: Conditions for DNA restriction reaction

Reagent	Concentration / Volume
EcoRI-HF	1µl
BamHI-HF	1µl
Cut-Smart Buffer	1X
DNA	2µg

Ligation was done with digested and purified pRXTN, PTEN-wt and PTEN-C124S constructs. Ligation was done as 3:1 (insert DNA:vector DNA) ratio. Insert mass calculation was done according to equation,

" Insert DNA mass (ng) = desired vector/vector molar ratio x vector mass (ng) x ratio of insert to vector lengths "

Ligation reaction was prepared according to **Table 14** and incubated at RT for 2 hours.

Table 2.33: Conditions for ligation reaction

Reagent	Concentration / Volume
T4 DNA Ligase	1µl
T4 DNA Ligase Buffer	1X
Vector DNA	0.020 pmol
Insert DNA	0.060 pmol

Total 100ng vector construct containing ligation reaction volume was used during transformation. 25µl C3040I *E. coli* strain was used for each transformation process.

Required volume of ligation volume added into *E. coli* C3040I strain. After 30 minutes incubation on ice heat-shock treatment was done at 42°C for 30 seconds. 800µl LB added into vector-*E. coli* mixture and incubated on shaker at 200rpm at 37°C while 1 hour. 200µl cell mixture spreaded onto the ampicillin containing LB-agar plate. Plates were incubated overnight at 37°C.

After incubation, single colony inoculation was done into ampicillin containing LB and LB volume was determined according to E.Z.N.A Midiprep Kit instructions. Colony inoculated LB incubated at 37°C overnight on shaker at 200rpm.

2.2.2 Cell culture maintenance of mouse and human cell lines

Cells were frozen in 1mL 50% FBS, 40% DMEM, 10% DMSO containing freezing medium for each vial at nitrogen tanks. Vials that were kept in nitrogen tanks were opened in FBS containing medium without penicillin-streptomycin. Mouse and human cell lines were cultured as **Table 15** and passages of cells were done according to ATCC instructions.

Table 2.34: Growth conditions for human and mouse cell types

Cell Types	Growth Conditions
HEK293T	High Glucose DMEM, 8% FBS, 1% Pen-strep, %1 Non-essential amino acid mixture
MEF	High Glucose DMEM, 8% FBS, 1% Pen-strep
PC3	RPMI, 8% FBS, 1% Pen-strep
DU145	RPMI, 8% FBS, 1% Pen-strep
BT549	RPMI, 8% FBS, 1% Pen-strep
MCF7	RPMI, 8% FBS, 1% Pen-strep
T47D	RPMI, 8% FBS, 1% Pen-strep

2.2.3 Adenovirus expressing Cre recombinase (AdCre) infection for α, $\beta^{+/+}$ MEF cells

Cells were seeded into 6-well plates. When cells were reached 20-30% confluency, medium was changed with 1% FBS containing medium. 3µl Adenovirus expressing Cre recombinase treatment was treated into each well and incubation was done for 6 hours at 37ºC. AdCre virus MOI was 10^{10} . After incubation, medium was removed and growth medium added into wells. AdCre treatment was done twice to increase efficiency.

2.2.4 Transfection of Human and Mouse Cell Lines

2.2.4.1 Stable Retroviral Transduction

Lipofectamine transfection was done for straight expressed vectors. Transfections were done on the 6-well plates and firstly viral particles were produced in HEK293T cells. Mix1 was prepared with 6µl lipofectamine 2000 reagent completed up to 250µl with empty DMEM and incubated for 5 minutes at RT. Mix2 contains 1µg gag/pol, 1µg vsv.g and 2µg plasmid of interest and volume completed up to 250µl with empty DMEM. Mix1 and Mix2 samples were mixed in 1:1 ratio and incubated while 20 minutes at room temperature. HEK293T cells' medium was changed with fresh medium and lipofectamine-plasmid mixture added into seeded cells, total volume was completed up to 2mL. After 24h incubation, medium was changed and after 48h first medium was collected. Also, another collection was done at 72h and supernatants were filtrated with 0.45micron filters. Polybrene added into filtrated medium as 8 µg/µl concentration.

Filtrated viral particle containing medium added onto the cells that seeded as 20% concentration. Cells were incubated with viral particle at least 6 hours at 37ºC and medium was changed with growth medium. Viral particle incubation was done at least 2 times. After viral particle treatments, cells undergo antibiotic selection according to selection markers of vectors.

2.2.4.2 Transient Transfection

Lipofectamine 3000 reagent was used for transient transfections. 250.000 HEK293T cells were seeded into 6-well plate per well. Mix1 was prepared with 6µl lipofectamine 3000 reagent and volume was completed up to 125µl with DMEM. Mix1 incubated at room temperature (RT) while 5 minutes. Mix2 was prepared with 2500ng DNA, 5µl P3000 reagent and 125µl DMEM. Then, Mix1 and Mix2 samples were mixed and incubated at RT for 15 minutes. After incubation, Mix1-Mix2 mixtures were added into each well and incubation with mixtures done at least 48h.

2.2.5 Cellular proliferation assay- Crystal violet assay

Cells were seeded into 12-well plates as 2000 cells/well and 6-well plates as 15000 cells/well confluency. Cells were seeded with their growth medium, after 24h incubation growth medium removed, inhibitor and 4% FBS containing medium added to cells. When control cells reached confluency, fixation solution was added to wells and fixation was done at least 2 hours. After fixation process, cells were washed with 1X PBS at one time and crystal violet stain added, incubation was done at least 1hour. Incubation was done for at least 30 minutes. After incubation, crystal violet stain was collected and washed with water for two times. Plates were air-dried. For measurement, destaining solution added into each well and wells incubated at RT for 1 hour. 200µl solution taken from each well and transferred to 96-well plates, measurements were done with spectrophotometer.

2.2.6 Protein Biochemistry

2.2.6.1 Harvesting Cells and Cell Lysis

After induction and incubation with our interest molecule, cells were collected with cell lifter on the ice. Cells growth medium was removed and washed with ice cold 1X PBS. PBS added into culture dish and cells were scraped with cell lifter. PBS that contains cells were collected into falcon tubes and centrifuged for 2500 rpm while 5 minutes at +4^{o}C. Supernatant was removed and pellet was snap-frozen.

For pellet lysis, lysis solution was prepared freshly and according to recipe at Table. Lysis buffer added into as 3x volume of the pellet and transferred into eppendorf tubes. Tubes were incubated on ice while 30 minutes and tubes were flicked during incubation. After incubation, tubes were centrifuged at 13000rpm while 15 minutes at +4^{o}C. After centrifugation, supernatants were collected and snap-frozen.

2.2.6.2 BCA Assay for Protein Concentration

Pierce BCA Protein Assay Kit was used for quantification of protein concentration. According manufacturer's manual, microplate procedure applied for protein concentration measurement. Regarding to our protein concentration levels of our cells, albumin standards were adapted to range between 0µg - 15µg BSA concentrations. 200µl working reagent and 25µl BSA or unknown protein solution were mixed on a plate shaker for 30 seconds. Incubation was done for 30 minutes at 37^{o}C and absorbance values measured with plate reader 562nm.

2.2.6.3 Sodium Dodecyl Sulfate Polyacrylamide Gel Electrophoresis (SDS-PAGE)

10% resolving gel and 4% Stacking gel was prepared according recipe at **Table 16**.

30ug protein loaded into gel. Gels run at 90volt for approximately 90 minutes. Nitrocellulose membranes were used for wet transfer process. Transfer buffer contains methanol for nitrocellulose membrane activation.

Table 2.35: SDS-PAGE gel components

	Stacking Gel (%4)	**Resolving Gel (10%)**
30% mixture of acrylamide/bisacrylamide	660µl	3.3mL
TEMED	5µl	5µl

10% APS	25µl	50µl
Stacking Buffer (pH=6.8)	1.26mL	-
Resolving Buffer (pH=8.8)	-	2.5mL
ddH_2O	3mL	4.1mL
Total Volume	**5mL**	**10mL**

Protein transferred nitrocellulose membranes were stained with Ponceau stain while 10 minutes at RT. Then membranes were washed with dH_2O.

3% BSA (w/v) in 1X TBS-T solution was used for blocking. Blocking process was done at +4ºC while 1 hour. After blocking step, membranes were soaked into primary antibodies at least overnight. Membranes were incubated with phosphor-specific antibodies for 2 days. After primary antibody incubation, membranes were washed with TBS-T for 3 times while 10 minutes at RT. Proper HRP linked secondary antibody incubation was done to membranes at +4ºC while 2 hours. Membranes were washed with 1X TBS-T for 3 times while 10 minutes at RT again. Membranes were washed with dH_2O before visualization of membranes with ECL. ECL solutions were used according to manufacturer's protocol and visualization of membranes were done with Amersham Imager 600.

2.2.7 mRNA analysis

2.2.7.1 RNA isolation

Cells pellets were collected and trizol reagent added to cell pellets according to their cell confluency. 500µl Trizol reagent added up to $5x10^6$ cells and 1mL Trizol reagent added up to $1x10^7$ cells. RNA isolation was performed to Trizol containing cell pellets' with RNeasy Plus Mini Kit according to manufacturer's protocol. RNA concentrations were measured with Nanodrop.

2.2.7.2 cDNA synthesis

cDNA synthesis reactions were prepared from 1000ng RNA with BioRad iScript cDNA Synthesis Kit for each sample according to **Table 17**.

Table 2.36: Conditions for cDNA synthesis reaction

Reagent	**Concentration / Volume**
5X iScript Reaction Mix	4µl
iScript Reverse Transcriptase	1µl
RNA	1000ng
Nuclease free water	Up to 20µl

2.2.7.3 qPCR

cDNA template and primer template mixes were prepared according to **Table 18.** For each reaction 5µl cDNA template mix and primer template mixes added into each well.

Table 2.37: Conditions for qPCR reactions

	Reagent	**Concentration / Volume**
cDNA template mix (5µl)	cDNA	0.05µl (50ng)
	2x sybr green mix	0.5µl
	Nuclease free water	Up to 5µl
Primer template mix	2x sybr green mix	4.5µl
	10µM primer mix (forward + reverse)	0.4µl
	Nuclease free water	Up to 5µl

Table 2.38: Thermocycler conditions for qPCR reactions

	Temperature	Duration
Pre-Incubation (1 cycle)		
	95ºC	**10:00**
Amplification (40 cycles)		
	95ºC	**00:30**
	60ºC	**00:30**
	72ºC	**00:30**
Melting (1 cycle)	**95ºC**	**00:10**

2.2.8 *In silico* Analyses

Microarray data (GSE21543) was retrieved from NCBI (National Center for Biotechnology Information) Geo database [41]. GSE21543 dataset was separated into two groups as wt and transgenic. Wt group contains data from normal ventral prostate tissue and the transgenic group have data from ventral prostate tissue which shows mPIN (mouse prostatic intraepithelial neoplasia). Differential gene expression analysis was done in GEO2R (https://www.ncbi.nlm.nih.gov/geo/geo2r/) with Benjamini & Hochberg (False discovery rate) using 0.05 cut-off between two groups. Pathway enrichment analysis was done with David (https://david.ncifcrf.gov/summary.jsp).

The copy number alteration and survival analyses were done in cBioPortal across various cancer data (https://www.cbioportal.org/) [42]. Copy number alteration which contains amplification, deep deletion, fusion, missense mutations. Overall survival analysis was retrieved under comparison/survival tab for SQLE gene in both prostate and breast cancer studies separately.

ROC plotter (http://www.rocplot.org/) gives insight about link between gene expression and therapy response. Biomarker potential of SQLE gene is searched in response to relapse-free survival at 5 years for breast cancer data with tamoxifen endocrine therapy treatment.

2.2.9 Statistical Analyses

GraphPad Prism 6 was used to perform statistical analyses. Graphs were drawn by using GraphPad Prism 6. Two-tailed student's test was performed for the indication of significance between two groups.

Chapter 3

3 Results

3.1 Analysis of p110α and p110β Prevalence in Various Genetic Settings

3.1.1 Analysis of PI3K isoform prevalence in PTEN knock-down MEFs

Isoforms of PI3Ks play various roles in different cell lines and dependencies to PI3K isoforms differ from cell type to cell type **[43]**. Firstly, mouse embryonic fibroblasts (MEFs) were used because MEFs are untransformed and their cellular proliferation mainly depends on the p110α isoform compared to other PI3K isoforms. When BYL719 (p110α inhibitor) and KIN193 (p110β inhibitor) treatments were administered, MEFs proved to be more sensitive to p110α inhibition, in accordance with previous reports [44] **(Figure 3.1A)**.

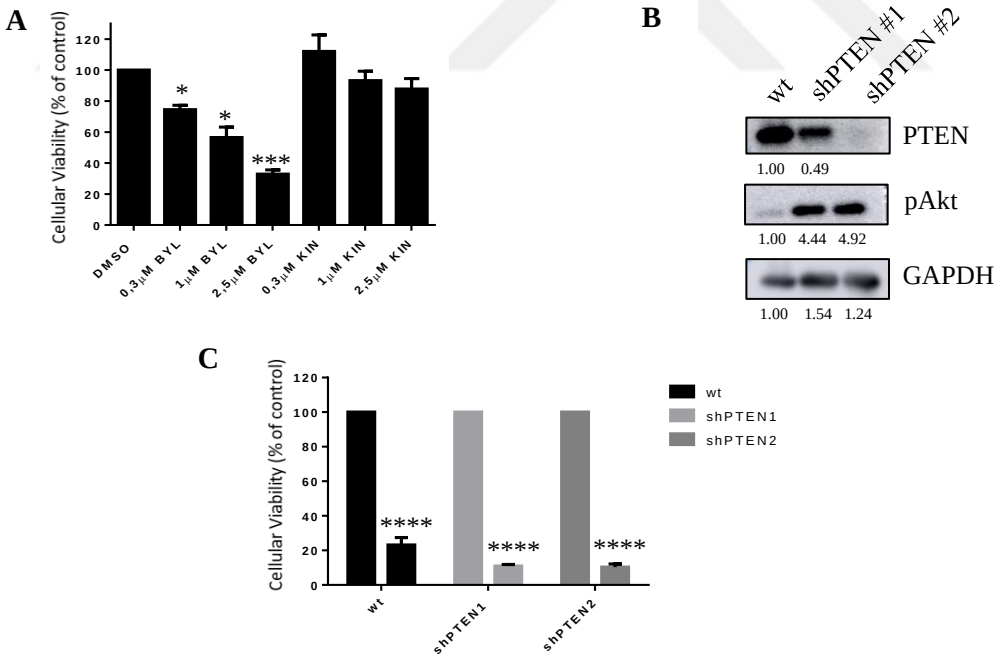

Figure 3.1: MEFs mainly depend on p110α for cellular proliferation and require class Ia PI3Ks in the absence of PTEN. **A)** Crystal violet assay quantification for BYL719 and KIN193 treated MEFs with increasing dosage. **B)** 2 different shPTEN constructs were used to stably knock down PTEN expression via lentiviral

transfections. Harvested cells were used for immunoblots and PTEN, pAkt (S473) levels were determined. **C)** AdCre treatments were done twice for α,$\beta^{+/+}$ MEFs and their proliferation rates were measured with crystal violet assay. Quantification of crystal violet staining results were measured for AdCre treated MEFs,*p<0.05, ***p<0.005, ****p<0.0001 (error bars show standard deviation in three independent experiments).

Cross cancer genomic studies exhibited that 30% of tumor samples bear PTEN loss [22]. Interestingly PTEN-loss induced tumorigenesis allows cancer cells to become more dependent on p110β isoform instead of p110α [45, 46]. Molecular mechanisms responsible for this prevalence is currently unclear. Therefore, we wished to investigate the impact of PTEN loss on isoform dependence in MEF cells. PTEN expression was ablated with two different shRNA constructs. shRNA plasmids were introduced into cells via lentiviral transduction. Anti-PTEN immunoblots were conducted to demonstrate PTEN knock-down efficiency. According to our results, shPTEN #2 construct has a higher PTEN knock-down efficiency compared to shPTEN #1 **(Figure 3.1B)**. Concomitantly an increase in the phosphorylation of Akt was observed with PTEN shRNA treatments because PTEN activity restrains the PI3K pathway **(Figure 3.1B).** In the presence of diminished PTEN expression, we set out to determine whether MEFs still depend on the p110α isoform. Genetically engineered α,$\beta^{+/+}$ MEF cells were used which harbor LoxP sites within the first exons of *PIK3CA* and *PIK3CB* genes. With Cre-recombinase expressing Adenoviral transduction (AdCre), *PIK3CA* and *PIK3CB* genes were simultaneously floxed and p110α, p110β double knock-outs were generated. With crystal violet assay, viability of AdCre treated cells decreased significantly compared to mock treated controls **(Figure 3.1C)**.

Our results implicated that PTEN knock-down did not rescue the growth defects imposed by knock out of ubiquitously expressed class IA PI3K isoforms. Cells still appear to require class IA PI3Ks for proliferation in the absence of PTEN. The interesting question however remained, did PTEN abolishment caused any dependence change in PI3K isoforms? To determine whether loss of PTEN induced a shift in isoform dependence, shPTEN expressing MEFs were treated with isoform-specific PI3K small molecule inhibitors. shPTEN-#2-MEF cells, which displayed a better knock down efficiency of PTEN, were shown to be more resistant to high doses

of p110α inhibition treatment compared to wt-MEF and shPTEN-#1 MEF cells **(Figure 3.2A)**. These results implicate that the extent of MEF cells' dependency on p110α is determined by PTEN levels. However, sensitivity to p110β inhibition did not change for both shPTEN-MEF lines.

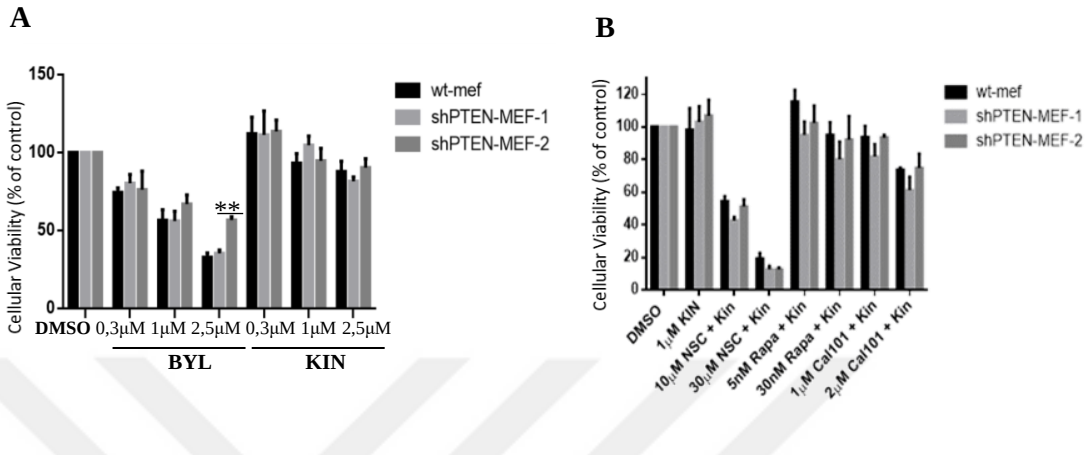

Figure 3.2: Cellular viability of PI3K inhibitor treated shPTEN-MEF cells. A) shPTEN transduced MEFs were treated with 0.3, 1 and 2.5μM BYL719 or KIN193 for crystal violet assay. Quantifications were done for inhibitor treated shPTEN-MEFs. ***p<0.005. **B)** 10, 30μM NSC, 15, 30nM rapamycin and 1, 2μM Cal101 treatments were done for shPTEN MEFs (error bars show 3 independent experiments that bear standard deviation).

Because PTEN knock down did not induce a change in p110β isoform dependency but a partial decrease in p110α dependency, we set out to combine this with other pharmacological inhibitors of PI3K pathway to accentuate subtle differences. Therefore, various small molecule inhibitor treatments were performed to display change of isoform dependence into p110β. In similar proliferation assays, p110β inhibitor was combined with PI3K pathway-related small molecule inhibitors like NSC23766 (Rac1 inhibitor), rapamycin (mTOR inhibitor), Cal101 (p110δ inhibitor). These inhibitor combinations did not lead to changes in sensitivity between control and shPTEN treated MEFs in a statistically significant manner **(Figure 3.2B)**.

3.1.2 Analysis of PI3K isoform prevalence in p110β overexpressed MEFs

PI3Ks are generally amplified or mutated in human cancer. Activating mutations of *PIK3CA* are observed in patients, but this is not the case for the other PI3K isoforms [47]. p110β, δ and γ isoforms have tumorigenic potential when they are in overexpressed as wild-type proteins [47]. For instance, p110β overexpression in prostate tissue leads to prostatic intraepithelial neoplasia (PIN) [41].

Exogenous p110β-wt expression was carried out in MEFs to understand whether upregulation of p110β-wt induces a shift in isoform prevalence from p110α to p110β. 1-2μM BYL719 and KIN193 were used in proliferation assays. We did not observe any change in sensitivity or resistance to BYL719 and KIN193 treatment upon exogenous expression of p110β in MEFs. MEFs appeared to be more dependent on p110α and less on p110β regardless of elevated p110β expression. 1μM GDC0941 and 2μM MK2206 inhibitors were used as positive controls as they target all PI3K and Akt isoforms respectively. Since the PI3K pathway is blocked more completely under these conditions, we observed a lower proliferation rate in both cell lines **(Figure 3.3A,B)**.

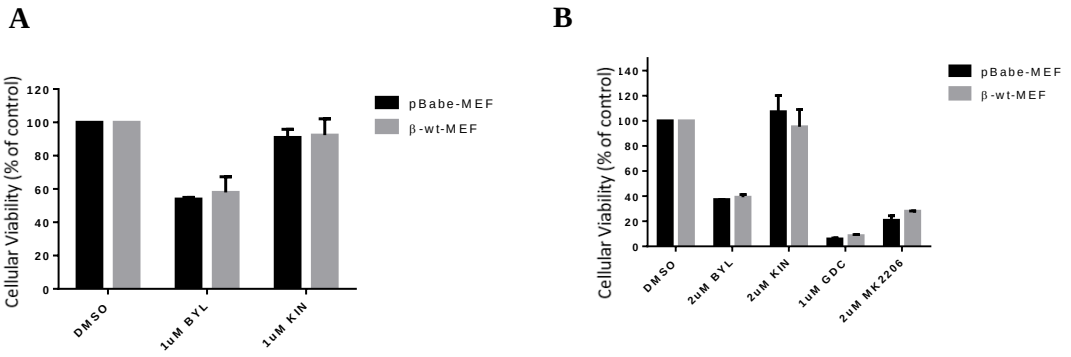

Figure 3.3: p110β overexpression did not cause any shift in isoform prevalence in MEFs. A) Quantification of crystal violet assays for BYL719 and KIN193 treated MEFs that express empty and β-wt vectors. **B)** Cell viability percentage for p110β overexpressed MEFs with treatments of BYL719, KIN193 and GDC0941 inhibitors with increased dosage (error bars show standard deviation in 3 independent experiments).

For understanding whether PI3K isoform prevalence is determined by more than one genetic component, we overexpress p110β in the absence of PTEN. Along these lines, we transfected p110β-wt in shPTEN-MEFs and performed proliferation experiments using isoform specific inhibitors. In general, shPTEN-MEFs appear to be much less dependent on p110α for proliferation. When PTEN knock-down is combined with p110β overexpression, p110α dependence is reduced even further. However, these cells still did not become significantly more dependent on p110β at moderate levels of inhibition **(Figure 3.4B)**. When higher dosages of 2μM BYL719 and 5μM KIN193 inhibitors were used, p110β overexpression leads to partial resistance to p110α inhibitor treatment. Also, overexpression of p110β-wt increased the sensitivity of MEFs to the p110β inhibitor compared to empty vector treated MEFs **(Figure 3.4C)**. In addition to these results, we even observed a trend towards resistance in GDC0941 treatment although it is not statistically significant. According to literature, GDC0941 inhibitor is only modestly effective towards p110β and γ isoforms compared to p110α and δ isoforms [48]. Less efficient inhibition ability of GDC0941 toward p110β overexpressing cells might be indicative of a dependence change towards p110β, which allowed the cells to proliferate in the presence of sustained p110α inhibition.

These results suggest that mere overexpression of p110β is not sufficient for making MEFs more p110β dependent. Likewise, knock-down of PTEN alone did not prove to be adequate to render cells more p110β dependent. On the other hand, combination of p110β overexpression and PTEN abolishment made cells more resistant to p110α and more sensitive to p110β inhibition. In the light of these results, in PTEN-null cancer cells, PTEN mutation and p110β overexpression might have occurred simultaneously beside other changes for making p110β the predominant PI3K isoform. However, these changes do not seem to be enough for a complete switch over.

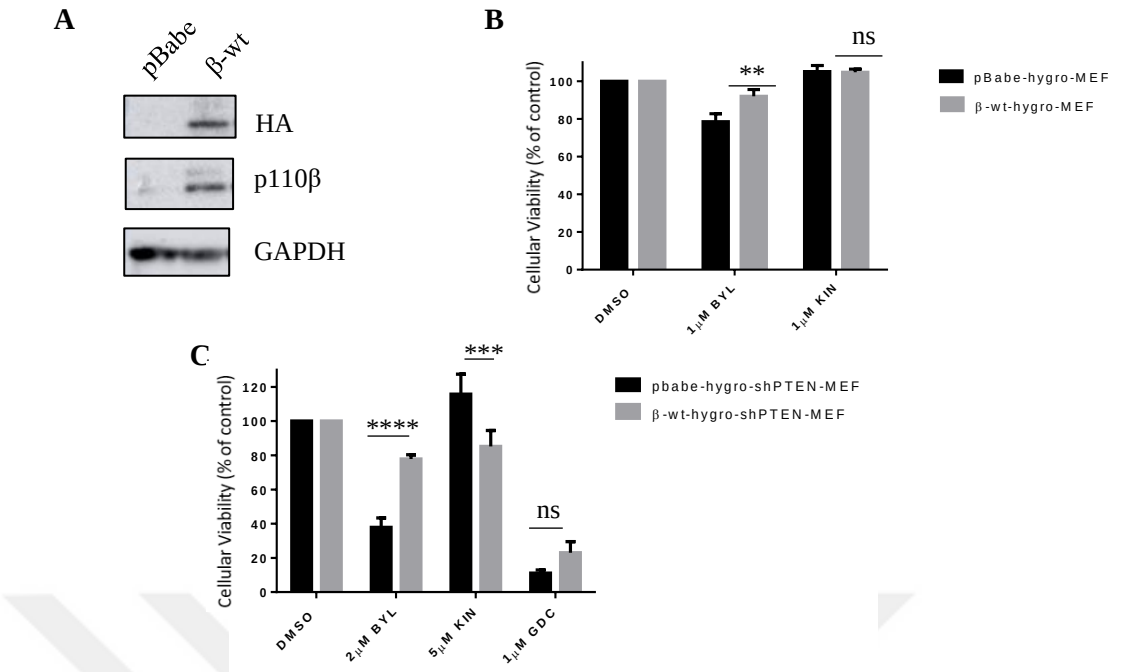

Figure 3.4: p110β overexpressed shPTEN treated MEFs gained resistance to BYL719 and sensitivity to KIN193 inhibitor. A) Immunoblot was analysed for shPTEN treated MEFs transfected with empty and β-wt vectors. **B)** Cellular viability for BYL719 and KIN193 treated shPTEN-MEFs were quantified. **C)** Crystal violet assay quantification were done for increased concentration of BYL719 and KIN193 treated shPTEN-MEFs **p<0.01, ***p<0.005, ****p<0.0001, ns (not significant) p>0.05 (standard deviation indicated with error bars from 3 independent experiments).

3.1.3 PI3K isoform prevalence in PTEN re-expressed PTEN-null PC3 cells

In the first part of the study, we down-modulated PTEN expression in untransformed MEFs to analyze isoform dependence. Our aim was to convert p110α dependence into p110β and partial changes were observed upon PTEN knock-down. In many cancer cell lines PTEN expression is diminished leading to PTEN loss and we wanted to utilize PTEN loss models to re-establish PTEN expression. We aimed to find out whether isoform prevalence would change from p110β into p110α in PTEN-null cells with PTEN re-expression. We sought an alternative cellular model to study PI3K

isoform prevalence and decided to use the PTEN-null PC3 prostate cancer model, p110β isoform has a dominant role in the proliferation of PC3s that is a metastatic prostate cancer cell line [45]. To see the impact of PTEN re-expression on PI3K isoform dependence, PTEN-wt and catalytically inactive PTEN-C124S mutant were stably expressed in PC3s **(Figure 3.5A)**.

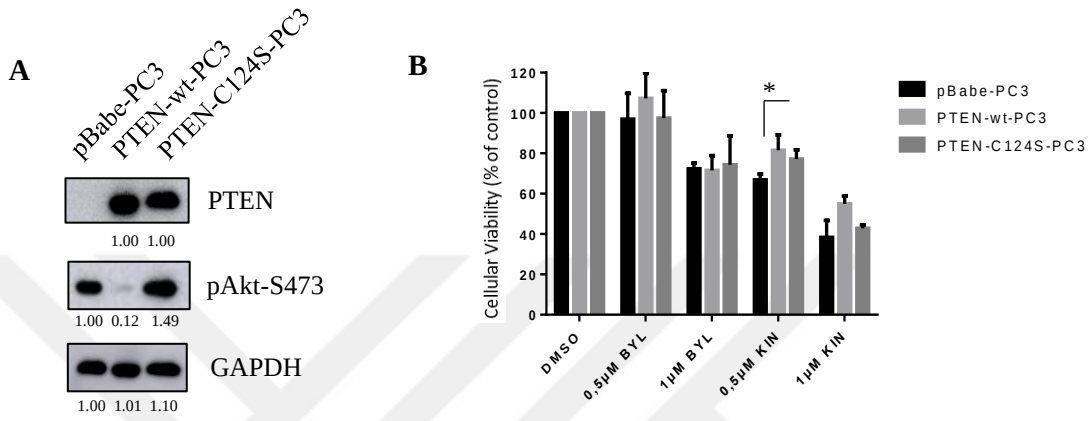

Figure 3.5: PTEN re-expressed PC3s became more resistant to KIN. A) Western blotting analysis was done for empty vector, PTEN-wt and PTEN-C124S expressed PC3s. **B)** Quantification of crystal violet assay for BYL719 and KIN193 treated empty vector, PTEN-wt and PTEN-C124S expressed PC3s *p<0.05.

pAkt levels were decreased when PTEN-wt was re-expressed in PC3s indicating pathway inactivation, but such a decrease in pAkt was not observed in catalytically inactive C124S mutant expressed cells. Because of the catalytical inability of the C124S mutant, PTEN could not perform its function as the PI3K pathway inhibitor. This result implicates tight correlation of phosphatase function of PTEN with PI3K pathway **(Figure 3.5A)**. According to crystal violet assay results, PTEN-wt add-back cells have acquired partial resistance to KIN193 treatment, but this is not the case for the PTEN-C124S mutant or empty vector treated PC3s. On the contrary, there was no gain of sensitivity or resistance to the p110α inhibition upon PTEN re-expression in PC3 cells **(Figure 3.5B)**.

3.2 Candidate genes which might cause PI3K isoform dependence

In MEFs with PTEN expression abolishment, p110α dependence decreased but there was no change in p110β dependence. In PC3s upon PTEN re-expression, cells become less sensitive to p110β inhibitor treatment but we did not observe a corresponding increase in sensitivity for p110α inhibitor treatment. Although PTEN expression level affects the dependence changes in p110 isoforms, we could not see a complete shift in isoform dependence in both MEF and PC3 cells. PTEN status and p110β overexpression do not appear to be the sole determinants for ClassIA PI3K isoform prevalence in these cellular models. In case the isoform prevalence is not determined by a single alteration, a series of changes might be necessary to impose PI3K isoform dependence.

PI3K pathway is important for cellular metabolism and studies claimed that different isoforms of PI3K regulate distinct metabolic processes: e.g. p110α has an important role in insulin signaling, whereas glucose homeostasis requires involvement of p110β [49, 50]. In addition to these, cholesterol pathway represents a major metabolic route, which is both critical for cellular integrity as well as lipidation of membrane associated proteins post-translationally. This lipidation might have a role in predominance of p110 isoforms because different p110 isoforms prefer different small GTPases, e.g. p110β-Rac and p110α-Ras interactions. These preferences localize p110 isoforms to different cell membrane microdomains [51]. Hence, we decided to look at metabolic changes that might alter cellular state, making the cells more prone to the action of a particular PI3K isoform. To understand which molecules might be involved in this process, we analyzed the microarray GEO dataset GSE21543 with GEO2R and DAVID 6.8 [52, 53]. GSE21543 dataset consists of microarray expression data from four wild type and four transgenic p110β mice. Transgenic p110β mice have PIN formation at the ventral prostate by constitutively active p110β isoform. In this model, constitutively active p110β is produced with addition of myristoylation tag to the N-terminal *PIK3CB* gene that containing androgen responsive cassette to restrict transgene expression to prostate tissue [41].

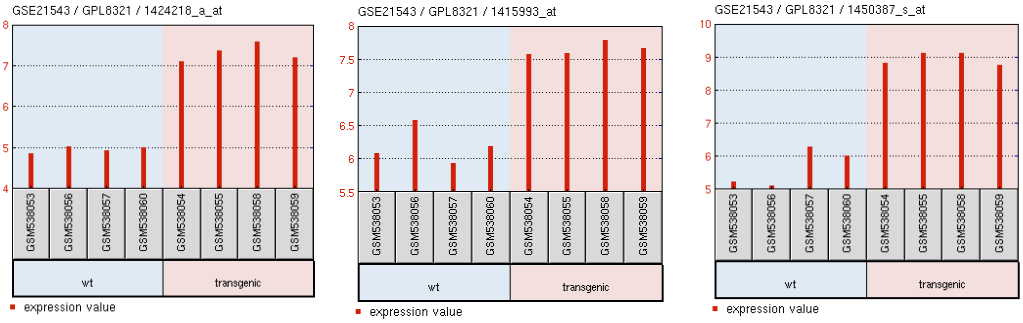

Figure 3.6: Metabolism related genes with a selective enrichment in GSE21543 dataset analyzed with GEO2R. Candidate genes' expression values and log fold changes (logfc) were analyzed with wt and transgenic mice results. Logfc values were calculated with GEO2R; CREB3L4 (Cyclic AMP-responsive Element Binding Protein 3 Like 4) logfc: 2.36**,** SQLE (Squalene Epoxidase) logFC: 1.46, AK4 (Adenylate Kinase 4) logFC: 3.29**.**

After GEO2R and pathway enrichment analyses on the GSE21543 dataset, we came across several genes that are involved in various metabolical processes. Through metabolic processes, we mainly focused on cholesterol pathway, energy metabolism and transcriptional regulation. SQLE, AK4 and CREB3L4 mRNA levels are significantly upregulated in the ventral prostate of p110β transgenic mice compared to wt in the GSE21543 dataset **(Figure 3.6)**. Squalene epoxidase (SQLE) is the second rate limiting enzyme in cholesterol synthesis pathway. SQLE gene expression is highly upregulated in cancerous tissue and some studies showed that SQLE promotes growth and metastasis progression [54, 55]. Adenylate kinases play key roles in ATP metabolism, catalyzes ADP formation from ATP and AMP. However, adenylate kinase 4 (AK4) does not have any kinase activity. AK4 is localized in the mitochondrial matrix and rather interacts with ADP/ATP translocase [56]. This unique member of adenylate kinase family was studied in lung, breast cancer. Metastatic tumors have higher expression of AK4 and it promotes tumor growth and invasion [56]. CREB family consists of transcription factors which are highly phosphorylated in various cancer. Cyclic AMP-responsive element binding protein 3 like 4

(CREB3L4) is highly expressed in prostate and interacts with androgen receptor which is important for prostate proliferation. Also, CREB3l4 gene is analyzed in both breast and prostate cancer studies [57, 58].

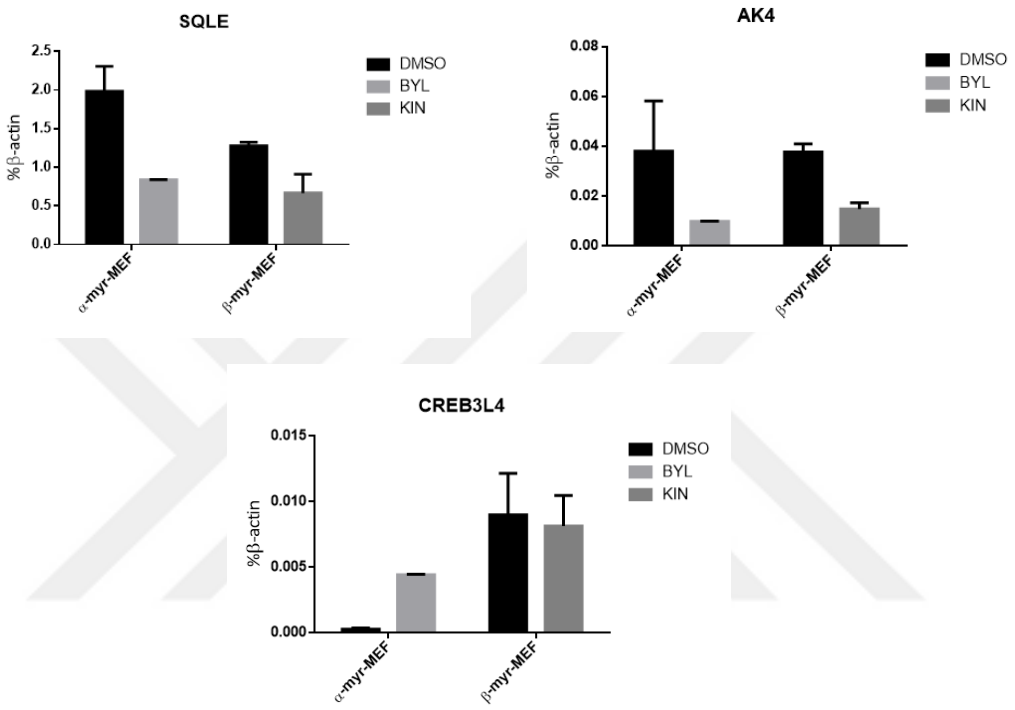

Figure 3.7: mRNA levels for candidate genes in MEFs with ClassIA PI3K inhibitor treatment. A) mRNA level changes were quantified when PI3K inhibitors used for MEFs. **B)** wt-MEF and myristoylated p110α, p110β cells were used for mRNA level quantifications. p110 isoform specific inhibitors were used for effect of p110 isoforms on candidate genes.

After analysis of the GSE21543 dataset, we wanted to investigate *CREB3L4*, *AK4* and *SQLE* expression alterations in constitutively activated p110 expressing MEFs. Addition of myristoylation tag to *PIK3CA* and *PIK3CB* genes leads to constitutive

activation of the PI3K pathway and cells become dependent on the myristoylated p110 isoform. When myr-MEFs were treated with their specific inhibitors, mRNA levels for both SQLE and AK4 were decreased. These results indicate that expression of *SQLE* and *AK4* genes appear to be under the control of constitutively activated PI3K isoform in MEFs. β-actin normalized CREB3L4 mRNA levels in MEFs were so low to draw proper conclusions **(Figure 3.7)**.

CREB3L4 mRNA levels were very low in comparison to β-actin levels, which ruled out precise quantification of these transcripts. So, we did not continue with analyzing CREB3L4 expression. According to GSE21543 and qPCR analyses, PI3K activation increases mRNA levels of *AK4* and *SQLE* genes. Since AK4 does not have any known kinase activity [59], we decided to focus on the cholesterol synthesis pathway, namely on SQLE because it represents an actionable target for inhibition. In addition to these, according to simvastatin sensitivity studies on PTEN-null and PTEN-wt cancer cells, we added HMGCR analyses to our results [60]. HMGCR is the first rate limiting enzyme in cholesterol synthesis pathway and it is inhibited by statins [60].

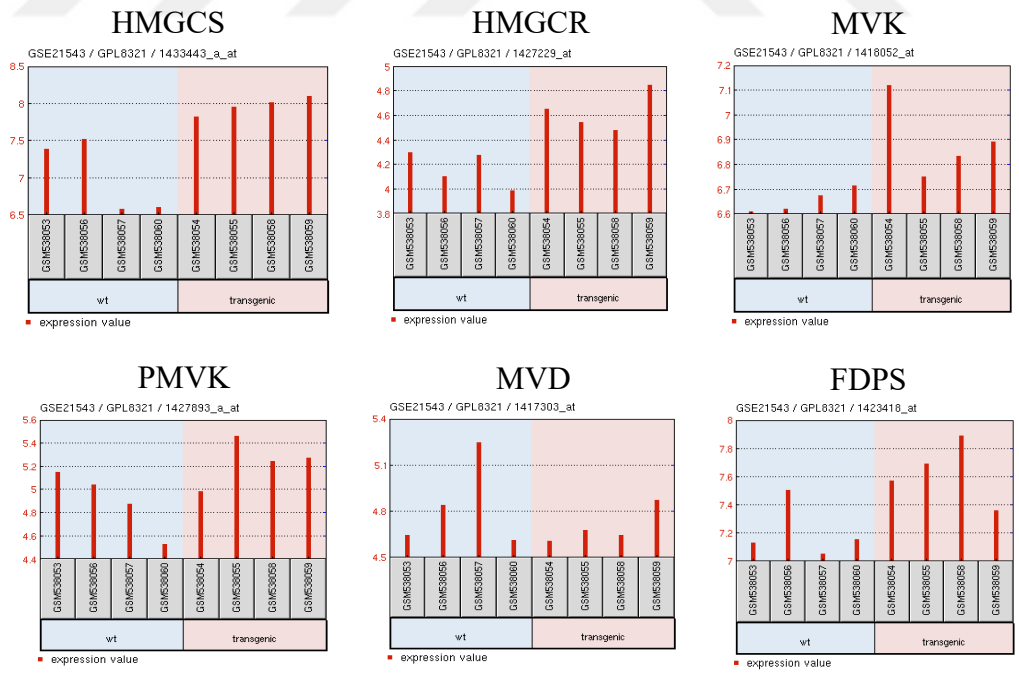

Figure 3.8: Expression levels of cholesterol pathway related genes in GSE21543 dataset. Graphs were prepared with GEO2R analysis. HMGCS (logFC:0.95), HMGCR (logFC:0.46), MVK (logFC:0.24), PMVK (logFC:0.34), MVD (logFC:-0.13) and FDPS (logFC:0.42) genes expression levels were retrieved from both wt and p110β myristoylated mice.

PTEN-status/PI3K activity may define a metabolic vulnerability towards cholesterol synthesis pathway. We investigated whether PTEN expression/PI3K activation affect expression of other cholesterol synthesis pathway enzymes, as well. To investigate this, the expression status of other enzymes taking part in cholesterol synthesis in GSE21543 data were analyzed with GEO2R. Analyzed genes in general, tend to have higher expression values in constitutively active p110β expressed mice prostate tissue compared to wt-mice results except for MVD **(Figure 3.8)**.

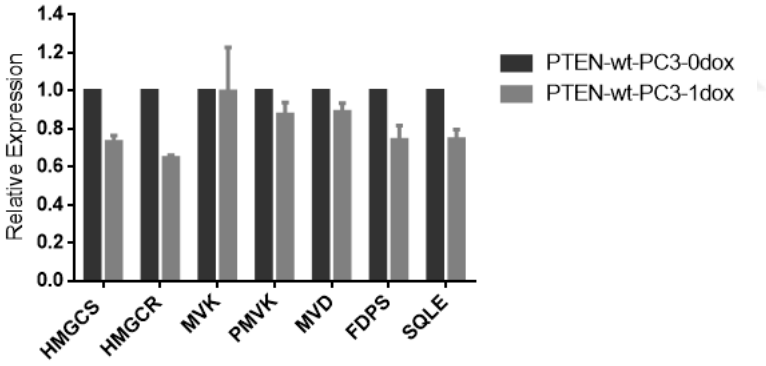

Figure 3.9: mRNA levels of cholesterol pathway related genes were affected with PTEN induction in PC3s. PC3 cells were induced with doxycycline for 6 days and mRNA levels for cholesterol synthesis genes were quantified.

According to the GSE21543 dataset, mRNA levels of HMGCS, HMGCR, MVK, PMVK and FDPS are also upregulated from constitutive activation of p110β beside the SQLE. We wanted to confirm our GSE21543 dataset analysis with an alternative method. Therefore, we analyzed corresponding mRNA levels in PTEN inducible PC3s. This approach might give more insight to PTEN interaction with cholesterol synthesis directly by regulated re-expression of PTEN in a PTEN null genetic background. Cholesterol synthesis pathway genes' mRNA levels were measured in PC3 cells upon PTEN induction for 6 days. According to qPCR results, HMGCS, HMGCR, FDPS, PMVK, MVD and SQLE mRNA levels tend to decrease with PTEN induction except for the MVK gene **(Figure 3.9)**. This data indicates that there was an inverse correlation between PTEN expression/PI3K activity and mRNA levels of cholesterol pathway synthesis enzymes.

3.3 *In silico* analysis of SQLE involvement in cancer

During tumorigenesis, cells are exposed to many epigenetic and genetic alterations. High amplification of certain genes is implicated as a hallmark of cancer and this can be critical for disease prognosis. Some of these genes which are related with poor prognosis are candidate for targeted therapies because cells become more sensitive to those gene inhibitions, a phenomenon described as oncogene addiction [61, 62]. For SQLE, we did bioinformatical analyses to see its potential in cancer progression. *SQLE* gene alteration ratio for major types of cancer was analyzed in cBioPortal [42]. According to this analysis, various cancers exhibit high *SQLE* alteration frequency. Prostate cancer has the highest amplification rate compared to other cancer types. Also, high *SQLE* gene amplification is seen in ovarian, colon and breast cancer which are mostly hormone-dependent cancers **(Figure 3.10A)**.

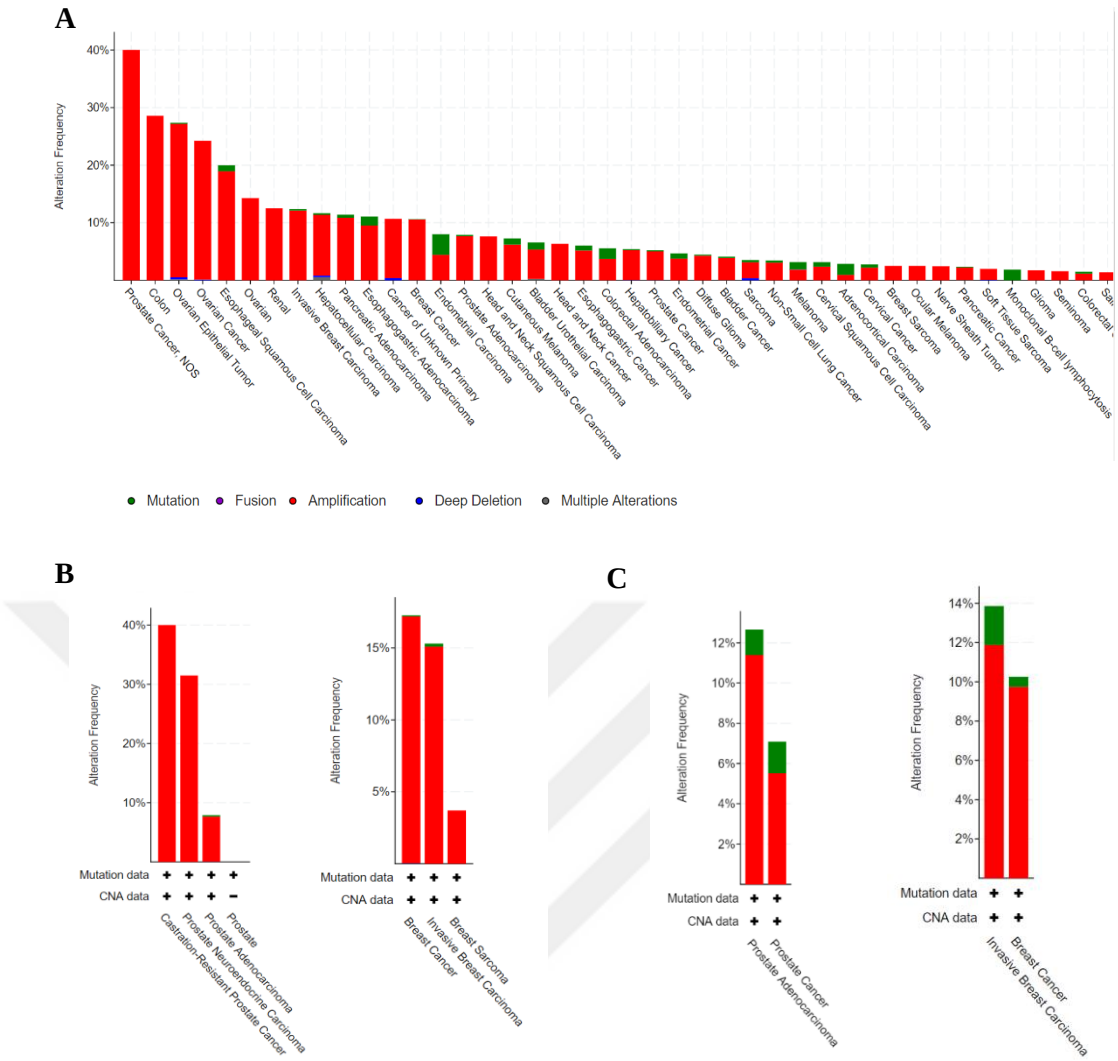

Figure 3.10: SQLE alteration frequency analysis results from cBioPortal. A) SQLE alteration frequency in different cancer types. **B)** SQLE alteration frequencies in breast cancer n=9531, prostate cancer samples n= 5192. **C)** PTEN-null prostate (n=203) and breast cancer tumors' SQLE alteration frequency (n=437).

Then, we focused on only breast and prostate cancer studies that exist on cBioPortal. Because alterations might happen at different stages of cancer progression such as primary and metastatic lesions. We wanted to investigate whether differential alteration rate of *SQLE* gene exists in different stages of cancer. Castration-resistant prostate cancer which do not respond to androgen deprivation therapy contains 40%

and prostate neuroendocrine carcinoma has 30% *SQLE* amplification respectively. Approximately 16% of amplification of *SQLE* occurs in breast cancer and 15% for invasive breast carcinoma. Breast sarcoma possesses lower rate of *SQLE* gene amplification **(Figure 3.10B)**.

Breast and prostate cancers have a high rate of PTEN-loss and downregulation of PTEN expression can occur via genetic, epigenetic and post-translational mechanisms [21]. We wanted to see whether SQLE and PTEN mutations exist in the same patients at the same time. For this purpose, PTEN mutated patient datasets were grouped and SQLE alteration frequency was analyzed. Amplification and mutation frequency is approximately 13% in prostate adenocarcinoma and 7% in prostate cancer. With breast cancer cBioPortal analysis, 14% amplification and mutation rate observed for invasive breast carcinoma and 10% for unclassified breast cancer **(Figure 3.10C).**

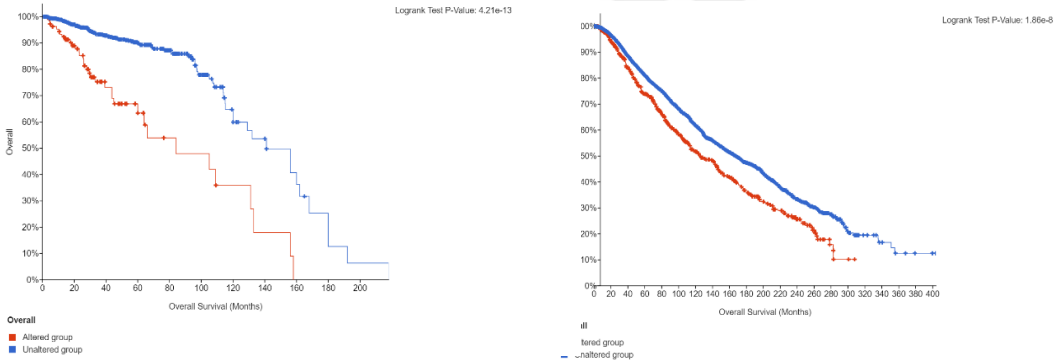

Figure 3.11: Overall survival rates prostate and breast cancer data with SQLE alteration in cBioportal. A) Prostate cancer patients showed significant decrease in survival in altered group (altered group n=114, unaltered group n=1359). **B)** Breast cancer patients have lower survival rate in altered group (altered group n=1057, unaltered group n=6486).

Also, overall survival rates were analyzed in SQLE altered and unaltered samples in cBioPortal. In prostate cancer, patients with SQLE amplification have lower survival rate compared to the unaltered patient group. The difference between survival rate is significant and p-value is $4.21e^{-13}$ **(Figure 3.11, left)**. In breast cancer, SQLE

amplification also predicts poorer survival as well with a p-value of $1.86e^{-8}$ **(Figure 3.11, right)**. Our analysis indicates that SQLE may have a role in breast and prostate carcinogenesis and affects patients' overall survival rates significantly.

3.4 Analysis of cholesterol synthesis pathway relation with PI3K in cancer cells

3.4.1 Simvastatin and terbinafine treatments for cancer cells

According to *in silico* and qPCR analyses, the cholesterol pathway might be implicated with the PI3K pathway. Cholesterol is precursor of steroid hormones and an important player in membrane biology contributing to the formation of lipid rafts. These membrane microdomains are critical for signal transduction [63]. Cholesterol synthesis is initiated by mevalonate production from HMGCoA molecules. During the synthesis of cholesterol, various by-products that are important for cell physiology are produced. These side products are important for prenylation a form of lipid post-translational modification [64].

In the cholesterol synthesis pathway, HMGCR and SQLE are two rate-limiting enzymes. We used small molecule inhibitors that selectively target these two rate-limiting enzymes. These small molecule inhibitors are simvastatin which is an HMGCR and terbinafine which is an SQLE inhibitor. Both simvastatin and terbinafine are FDA approved drugs, simvastatin is used as a cholesterol lowering drug and terbinafine is used against fungal infections. For understanding the effects of simvastatin and terbinafine in relation to p110 isoforms specific activity, myristoylated cell lines were treated with these inhibitors and cellular viability was measured.

α-myr-MEFs were not affected by simvastatin treatment in all used doses whereas β-myr-MEFs were sensitive to lower dose simvastatin treatment at 2μM and 5μM **(Figure 3.12, left)**. Likewise, β-myr-MEFs were more sensitive to terbinafine treatment in comparison to α-myr-MEFs **(Figure 3.12, right)**. Although α-myr-MEFs become more resistant to terbinafine treatment compared to wt-MEFs, simvastatin treatment did not lead to sensitivity change. On the other hand, β-myr cells have a sensitivity to both simvastatin and terbinafine treatment compared to the control group. Our results suggest that constitutive activation of p110β predisposes cells to

cholesterol synthesis pathway inhibitors. Also, according to literature raft mediated signaling is p110β dependent and if cholesterol synthesis inhibited, raft mediated signaling could have been compromised [60].

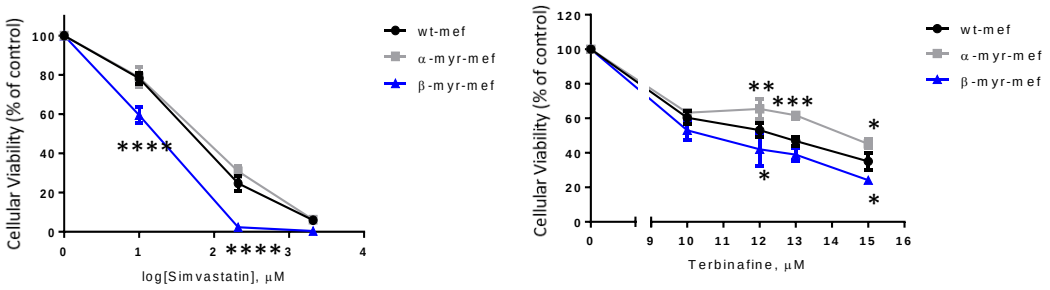

Figure 3.12: Cholesterol pathway inhibitor treatment for myristoylated p110 MEFs. Quantification for cellular viability percentage for ClassIA p110 isoform myristoylated MEFs that treated with simvastatin and terbinafine *p<0.05, **p<0.01, ***p<0.005, ****p<0.0001 (error bars is produced from three independent experiment with standard deviation).

According to the results obtained in shPTEN treated MEFs and PTEN re-expressed PC3 cells, PTEN expression status change leads to cells being less dependent on predominant PI3K isoforms e.g PC3s become more sensitive to p110β inhibitor and p110α inhibitor for MEFs. Also, SQLE expression levels were increased in p110β overexpressed mice as results of geo dataset analyses suggested and a corresponding increase in cholesterol synthesis pathway inhibitor sensitivity was observed in p110β-myr-MEFs. Besides these, PTEN have a pivotal role in cellular metabolism, e.g. glycolytic and cholesterol synthesis pathways. Studies showed that with PTEN loss might leads to an increase in glycolysis and fatty acid synthesis [65].

Hence, we wanted to investigate a possible involvement of PTEN in cholesterol synthesis. In order to study this, we used cholesterol pathway specific inhibitors in PTEN null or replete cancer cells. For this purpose, we used PTEN-wt and PTEN compromised breast and prostate cancer cell lines. According to PTEN status, PTEN-wt DU145 and PTEN-null PC3 prostate cancer cells were used. DU145 was more resistant to both simvastatin and terbinafine treatment compared to PC3s **(Figure**

3.13A). Accordingly, PTEN-wt MCF7 and PTEN-null BT549 breast cancer cell lines were used for inhibitor treatment. 5 and 10μM simvastatin led to significantly higher growth inhibition for PTEN-null BT549. MCF7 cells were more resistant to terbinafine treatment with all used concentrations **(Figure 3.13B)**. According to these results, both breast and prostate cancer cells that are PTEN replete were inherently more resistant to cholesterol synthesis pathway inhibitors compared to PTEN-null cell lines.

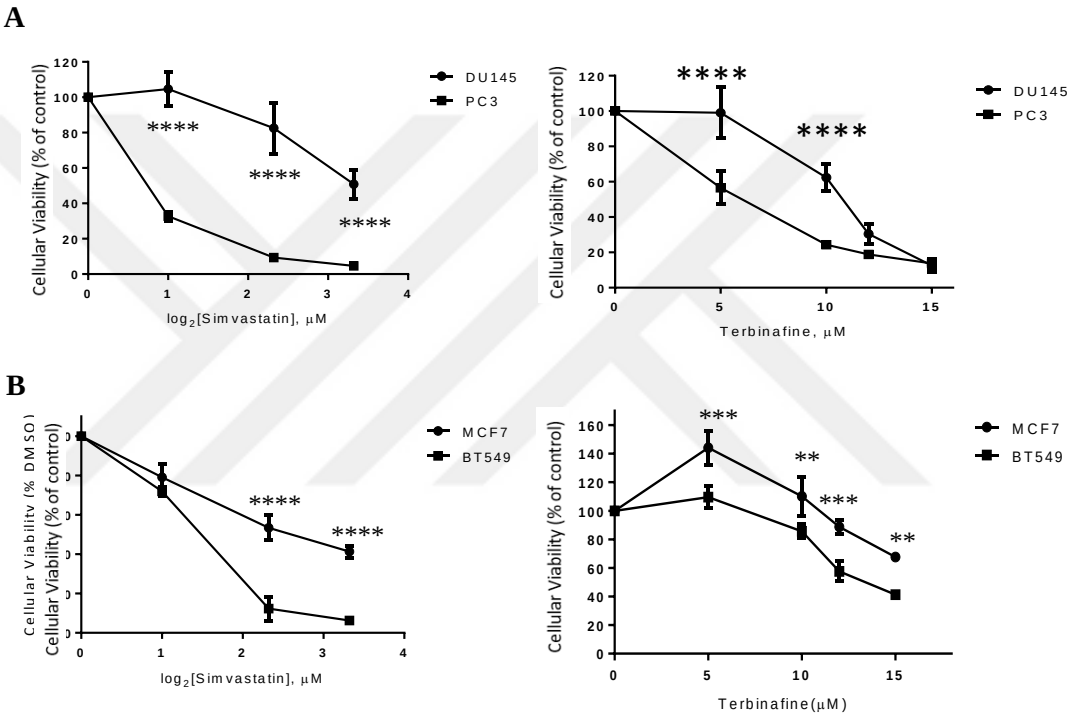

Figure 3.13: Prostate and breast cancer cells that have different PTEN status were treated with cholesterol pathway inhibitors. A) Cellular viability was quantified for simvastatin and terbinafine treated prostate cancer cells PTEN-wt DU145 and PTEN-null PC3. **B)** Cellular proliferation was assessed for breast cancer cell lines, PTEN-wt MCF7 and PTEN-null BT549 cells **p<0.01, ***p<0.005, ****p<0.0001 (error bars show 3 independent experiments that bear standard deviation)

Then we wanted to find out if PTEN reexpression would render isogenic cancer cells more resistant to cholesterol synthesis inhibition. To do this, we aimed at generating a PTEN inducible cellular cancer model. To that end, PC3 cells were transfected with pRXTN-PTEN-wt overexpression vector. PTEN-wt inducible PC3 cells were induced with 1μg/mL doxycycline for 6 days to express PTEN in PC3 cells. To see the induction efficiency of our cellular system, PTEN levels were measured in anti-PTEN and anti-GAPDH immunoblots and increased significantly with dox induction compared to uninduced PC3s **(Figure 3.14A)**. Simvastatin inhibitor treatment efficiency did not change upon PTEN reexpression and PTEN re-expressing cells did not gain any resistance to simvastatin. Whereas terbinafine treated PTEN expressed PC3 cells became partially resistant to the treatment **(Figure 3.14B)**. The effects of terbinafine treatment to PTEN expressed cells were less pronounced compared to the differences that were observed in PTEN-null and PTEN-wt cell lines in Figure 3.11. Since PTEN re-expression was done for short-term, this might cause sensitivity differences because metabolic reprogramming might need a longer time.

HMGCR inhibition does not only inhibit cholesterol synthesis but also blocks some other critical synthetic pathways like prenylation signals, ubiquinone that plays role in the electron transport chain [66]. PTEN addback might not be able to rescue those dependencies. Therefore, we thought that PTEN might not directly involved in regulation of HMGCR, simvastatin inhibition phenotypes differ in PTEN-null and PTEN-wt cells based on inhibition of downstream genes like SQLE.

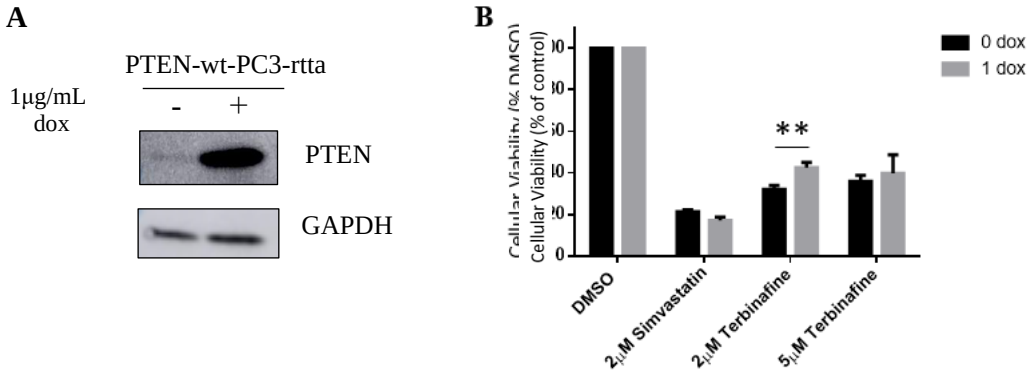

Figure 3.14: Prostate and breast cancer cells that have different PTEN status were treated with cholesterol pathway inhibitors. A) Anti-PTEN and anti-GAPDH immunoblots were prepared for quantification of level of PTEN expression **B)** Cellular viability for induced and uninduced PTEN-wt-PC3s were quantified **p<0.01, (error bars show 3 independent experiments that bear standard deviation).

Breast and prostate cancer cells have differential sensitivity to simvastatin and terbinafine treatments according to their PTEN status. Then we did some biochemical analyses to identify possible differences that could explain the correlation between PTEN status and cholesterol pathway. 5-10µM simvastatin and 10-15µM terbinafine treatments were done for both PC3 and DU145 cells for 2 days. After inhibitor treatments, PI3K, mTOR and apoptotic pathway related markers were analyzed in immunoblots. In the context of mTOR pathway, we did not observe any change in phosphorylation levels of p70 S6 kinase levels for both cell lines. However, when we looked at the phosphorylation sites of S6 ribosomal protein, we observed a decrease in phosphorylation levels with simvastatin treatment only in PTEN-null PC3s **(Figure 3.15)**. p70 S6 kinase phosphorylation site of mTOR (S2448 levels) were not changed with treatment **(Figure 3.16)**.

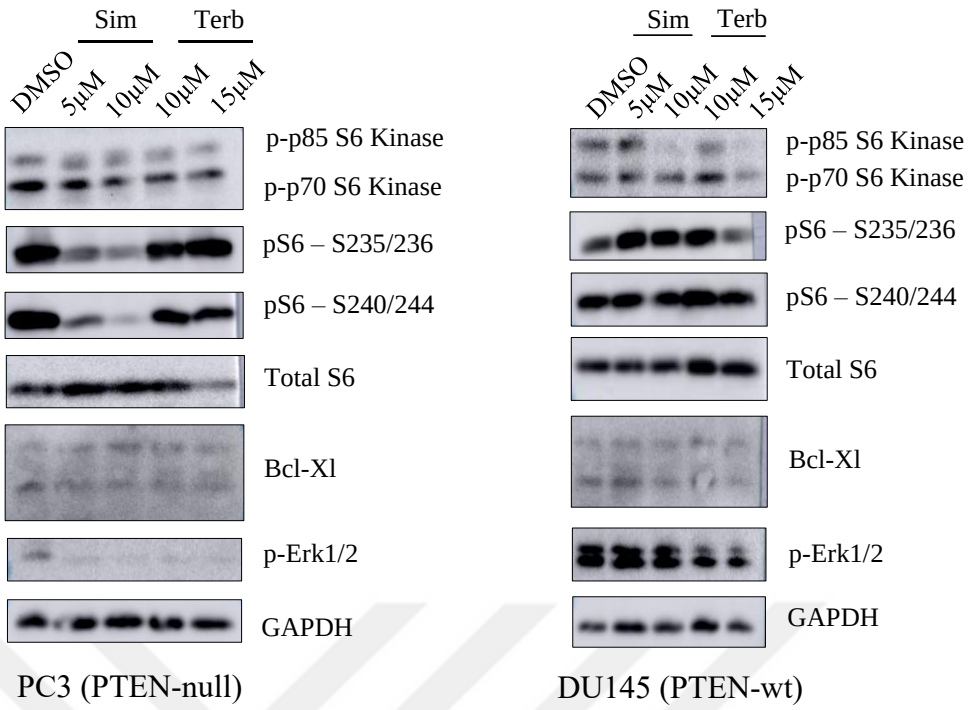

Figure 3.15: Regulation in PC3 and DU145 cells were affected differentially from simvastatin and terbinafine treatments. PTEN-null PC3 and PTEN-wt DU145 cells were treated with different concentrations of simvastatin and terbinafine for two days. Left panel shows immunoblots for treatments of PC3 cells and DU145 cells' immunoblots were shown at right panel.

We analyzed anti-Bcl-xl level in immunoblots to see effects of terbinafine and simvastatin inhibitors in apoptosis. Inhibitor treatment did not lead to any changes in Bcl-xl levels which is an anti-apoptotic protein for both cell lines **(Figure 3.15)**. To analyze PI3K pathway activation in relation to cholesterol pathway inhibitor treatment, both phosphorylation sites of Akt and 4EBP1 were analyzed. There was a decrease in pAKT-T308 levels in PC3s whereas T308 phosphorylation site did not changed in DU145. Differential phosphorylation attitudes indicated differential sensitivities of PI3K activation in response to cholesterol synthesis pathway inhibitors. This trend was seen in phosphorylation of 4EBP1 levels, as well. Terbinafine treated samples in PC3s had lower p4EBP1 Ser65 levels, but there was no change in cholesterol synthesis inhibitor treated DU145 cells. On the other hand, PRAS40 phosphorylation was more pronounced in PC3 cells but Thr246 phosphorylation levels were not detectable in

DU145 cells **(Figure 3.16)**. pAkt-T308 and p4EBP1 might be differentially targeted in PC3 and DU145 cells. Our data implicate that the connection between PTEN-loss and cholesterol pathway sensitivity is reflected on specific PI3K downstream targets.

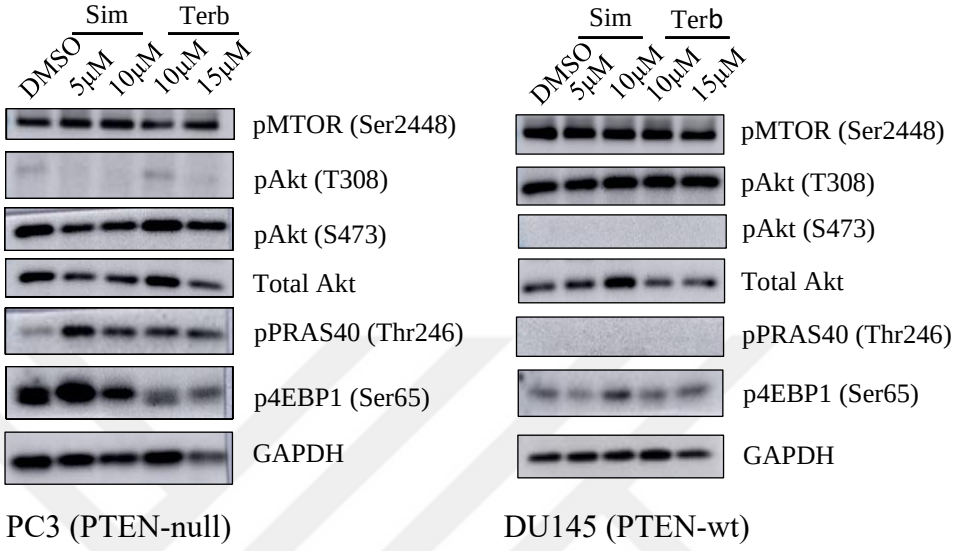

Figure 3.16: PI3K regulation in simvastatin and terbinafine treated PC3 and DU145s. Simvastatin and terbinafine treatments were applied to PTEN-null PC3 and PTEN-wt DU145 cells with different concentrations of for two days. Immunoblots were shown for PC3 and DU145 cells in left and right panel, respectively.

3.4.2 Biochemical analyses for PTEN-addback prostate cancer cells

Cellular viability experiments in breast and prostate cancer cells demonstrated that cells were resistant to simvastatin and terbinafine treatments in the presence of an intact PTEN. qPCR results implicated that, mRNA levels for cholesterol synthesis pathway genes were decreased upon PTEN addition. Then we analyzed protein levels of SQLE and HMGCS in anti-SQLE and anti-HMGCS immunoblots upon PTEN induction. Inducible wt PTEN was re-expressed in PC3 and LNCaP cells with 1μg/mL doxycycline for 6 days. On the left panel, HMGCS protein levels were not affected by PTEN expression induction for both PC3 and LNCaP cells **(Figure 3.17, left)**. With presence of PTEN protein, both PC3 and LNCaP cells have decreased SQLE levels compared to uninduced versions. For the Akt-S473 site that is a phosphorylation site of PDK1, we saw a decrease in induced PTEN-wt-PC3 and LNCaP cells because of

the catalytic activity of PTEN **(Figure 3.17, left)**. On the right panel, induction of PTEN expression levels were verified in immunoblots and we observed significant PTEN induction in all dox induced cells **(Figure 3.17, right)**.

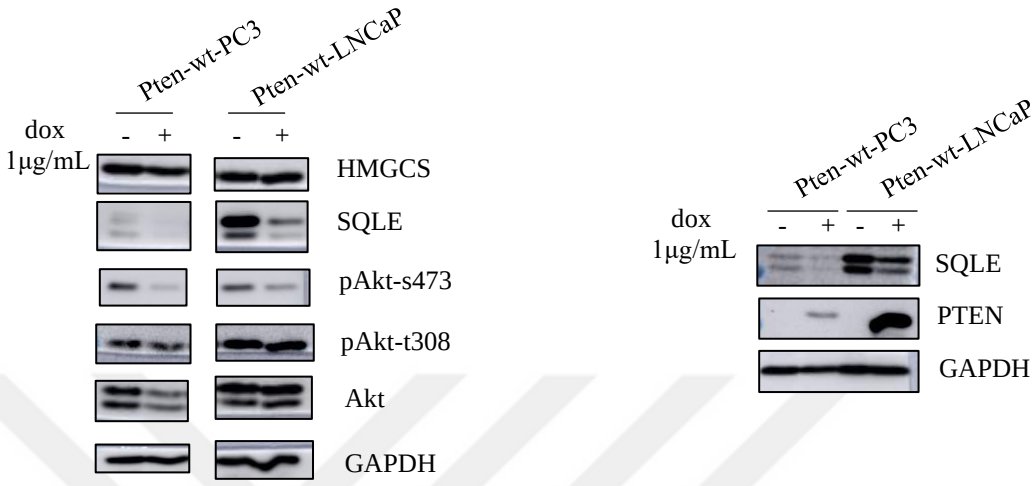

Figure 3.17: SQLE protein levels were affected from PTEN reexpression in prostate cancer cells. 1µg/mL doxycycline induction was done for wt PTEN addback PC3, LNCaP cells and for catalytically inactive PTEN expressed PC3s. Anti-HMGCS and anti-SQLE immunoblots were prepared for induced cells. Their phosphorylation levels of Akt were analyzed. Anti-Akt and anti-GAPDH blots were used for loading control. PTEN antibody was used for indication of doxycycline induction.

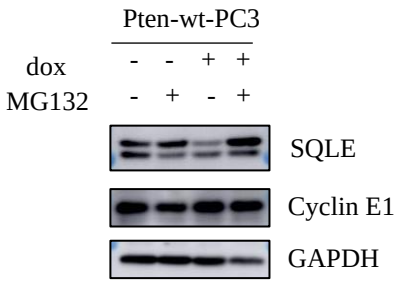

Figure 3.18: Proteasome inhibitor treated for doxycycline induced and uninduced PC3-PTEN addback cells. Anti-SQLE, anti-cycline1 and anti-GAPDH antibodies were used for MG132 treated PTEN-wt-PC3 cells. 10µM MG132 was treated while four hours to both doxycycline induced and uninduced PC3s.

PTEN reexpression upon doxycycline induction causes decrease in both SQLE mRNA and protein levels. Then we wanted to find out whether this down-regulation is achieved at only transcriptional or also at post translational level. To tease apart these possibilities we employed MG132 to prevent proteasomal degradation of proteins. With MG132 treatment, SQLE protein levels were accumulated instead of a decrease in samples which only expressed wt PTEN by doxycycline induction. In doxycycline induced PC3 cells, there was higher SQLE protein in MG132 treated cells compared to untreated cells. For uninduced cells, we did not see any difference between MG132 treated and untreated samples. So, we can say that the PI3K pathway, either directly or indirectly regulates protein stability of SQLE in addition to the previously mentioned transcriptional control **(Figure 3.18, left)**. This implicates a post-translational as well as transcriptional regulation of SQLE by PI3K pathway. Cyclin E1 protein is already quite stable in PC3 cells and MG132 treatment did not lead a further accumulation in its levels **(Figure 3.18)**.

3.5 Biomarker potential of SQLE in tamoxifen treated breast cancer

We wanted to understand biomarker potential of SQLE gene with datasets that contains patient data with endocrine and chemotherapy treatment. We investigated SQLE effect on relapse free survival rate of patients with different therapies using ROC Plotter [67]. Tamoxifen is an anti-hormone therapy agent used as a first line of treatment in ER positive breast cancer patients. According to our analyses, tamoxifen therapy responders have lower SQLE expression compared to non-responder patients. AUC value is 0.691 and p value is $3.1e^{-03}$ for SQLE **(Figure 3.19)**. AUC 0.691 value is classified as top quality for identifying SQLE gene as a biomarker predicting tamoxifen response in breast cancer patients [67].

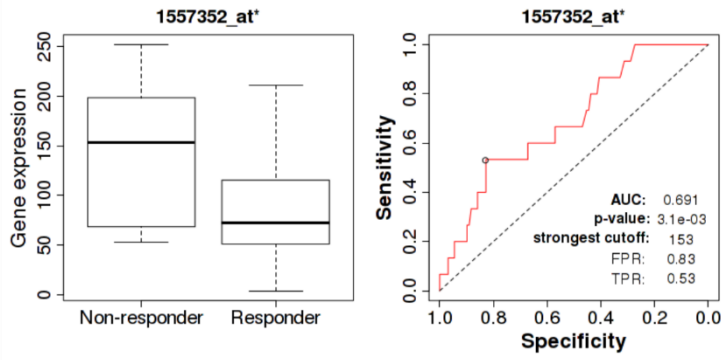

Figure 3.19: Higher SQLE expression is correlated with poor relapse free survival for tamoxifen treated patients. Box plot shows breast cancer patients (n=886) that taken tamoxifen endocrine therapy was analyzed. Non-responders contain n=127 and responders n=759 sample size. The area under the curve (AUC) is 0.691 for SQLE gene in tamoxifen therapy treated samples.

To see tamoxifen treatment effect on SQLE gene levels in cellular context, acquired resistance to tamoxifen was generated in breast cancer cellular models. PTEN replete ER+, PR+ T47D cells were exposed to high concentrations of tamoxifen for long term period and tamoxifen resistant T47D cells were produced [68]. Tamoxifen resistant breast cancer cells were biochemically analyzed. HMGCS1 protein levels were not affected by tamoxifen resistance in T47D cells which breast cancer cell line, but, SQLE levels were increased in T47D cells which became resistant to tamoxifen. Phospho pERK1/2 levels were increased upon response to anti-hormone resistance **(Figure 3.20)**. Since tamoxifen resistance cause upregulated expression of RTKs e.g. IGFR, HER2, ER, cells might become more dependent on MAPK to maintain cellular proliferation upon acquired tamoxifen resistance [69]. Of note, phospho pERK1/2 levels were found to be decreased in our PTEN-null PC3 cells and levels were stable in PTEN-wt DU145 cells **(Figure 3.15)**.

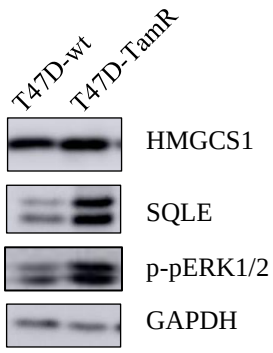

Figure 3.20: SQLE and HMGCS levels in T47D cells with tamoxifen resistant cell lines. Immunoblots for T47D and tamoxifen resistant T47D cells were shown at left panel. On the right panel, BYL719 resistant and wt T47D cells' anti-SQLE, anti-HMGCS and anti-GAPDH immunoblots were utilized.

Tamoxifen is highly used chemotherapeutic agent for breast cancer patients. After our *in silico* and *in vitro* analyses about tamoxifen resistance in breast cancer, SQLE seems to have a potential to be a biomarker gene upon tamoxifen resistance in breast cancer. SQLE targeting might be a potential combinational treatment option for tamoxifen. Also, SQLE might be important for other cancer types besides the PTEN-null cancers. So, these findings might be a lead for further investigations on SQLE and hormone dependent cancer types. Since also there is highly amplification of SQLE in ovarian cancer which is hormone dependent cancer type, according to our cBioPortal analyses (Figure 3.10).

Chapter 4

Discussion

PI3K pathway mutations are observed in many different cancer types. PTEN is one of the most frequently mutated genes and PTEN loss is observed in different tumor types like breast, prostate and ovarian cancer. In the absence of PTEN, p110β becomes the most prominent isoform among ClassIA PI3Ks. However, the mechanism that causes isoform dependence change in PTEN-null cancers is not clear. Pan-PI3K inhibitors were used for the treatment of PI3K activated tumors, but these inhibitors have wide side effects [70]. Instead, p110β isoform specific inhibitors like AZD8186, KIN193 were tested to treat PTEN-null cancer types [71, 72]. Single p110β inhibitor treatments caused transient repression of PI3K pathway and then cells became resistant to inhibition. Studies claimed that tumor cells which depend predominantly on either p110α or p110β, may become dependent on other isoforms of PI3K upon inhibitor treatment. According to a study, after p110β monotherapy treatment to PTEN-null cells, p110α isoform was activated via IGFR or other RTKs [73, 74]. On the other hand, to prevent possible feedback mechanisms, combinational therapies were used with p110β inhibitors. Src inhibitor and docetaxel which is a chemotherapy agent were used as combinational treatments for PTEN-null cancer types [71, 75]. Finding the mechanistic link between PTEN-null cancer and p110β dependence might improve current treatment regimens and lead to more effective repression of possible feedback mechanisms.

In this study, immortalized mouse embryonic fibroblasts (MEFs) were used firstly because of their untransformed nature and having wild type PTEN expression. In our experiments, we tried to observe whether cells are still in need of p110α and p110β for their cellular growth in the absence or presence of wild type PTEN. We found that in the face of efficient *PTEN* knock down, MEFs still need ClassIA isoforms for cellular growth. Dependencies to *PIK3CA* and *PIK3CB* genes were checked in shPTEN treated MEFs. Although PTEN repression did not cause sole isoform dependence change in MEFs, there was a decrease in predominant isoform dependence which is p110α (Figure 3.1).

Different isoforms of PI3Ks interact with different small GTPases regulating their activities. For instance, Ras protein interacts with p110α isoform and Rac provides activation of p110β isoform selectively. Because of these differences in interaction preference, we tried to combine Rac, mTOR and p110δ inhibitors with p110β inhibitor to see the effects of them on dependence change. However, according to our analysis, those genes did not turn out to play major roles in isoform predominance in MEFs.

Constitutive activation of wild type p110β able to induce PIN formation [41]. PIN is the first stage of prostate cancer and cells begin to enlarge into ducts and acini. To understand whether p110β overexpression leads to p110β dependence in cells, we overexpressed p110β in MEFs. There was not any change in isoform dependence from p110α into p110β. Then, p110β overexpression was combined with PTEN repression. The combination causes resistance to p110α inhibitor and sensitivity to p110β inhibitor. Also, when we look at GDC0941 treatment for p110β overexpressed MEFs in PTEN depleted background, cells showed a trend toward resistance to GDC0941 which is a pan-PI3K inhibitor. Because of the modest selectivity of GDC0941 towards p110β, we can say that PTEN depleted MEFs become more dependent on the p110β isoform. Only overexpression of p110β was not sufficient for making cells more p110β dependent (Figure 3.3).

In untransformed MEFs, we saw that PTEN and p110β expression changes had a partial effect on isoform predominance. PI3K pathway activation via PTEN suppression leads to a decrease in p110α dependence. Also, MEFs are of mesenchymal origin and we wanted to corroborate these findings in epithelial models of human cancer. We used PC3 cells which are PTEN-null. To see the effect of PTEN in a cancer cell line, we overexpressed wt PTEN and catalytically inactive PTEN in PC3s. Only, wt PTEN re-expression decreases dependence to p110β but we did not see any change in p110α dependence. Also, catalytically inactive PTEN expression did not cause any sensitivity to p110α or p110β inhibitor treatments (Figure 3.4). So, the catalytic activity of PTEN caused a dependence decrease to p110β for cellular viability.

According to MEF and PC3 results, PTEN status has a role in isoform dependence but it is not the sole determinant in this process. It causes a decrement in p110α dependence in MEFs and p110β dependence in PC3 cells. However further steps are required for fully-fledged switches in isoform dependence between ClassIA PI3K isoforms. For

understanding which genes might be involved in this process, we analyzed GSE21543 microarray dataset. The dataset consists of ventral prostate tissue expression values of genes upon expression of constitutively active p110β from early embryonic development. With GEO2R and David 6.8 online tool analyses, we mainly focused on the metabolic changes because in tumor microenvironment, cancer cells are in need of bulk amount of molecules and metabolites for their cellular growth and survival. We came across with AK4 which is involved in ATP-AMP homeostasis, SQLE which is a cholesterol synthesis enzyme, CREB3L4 is a transcription factor and inhibits adipogenesis. To confirm these *in silico* results in cells with constitutively activated PI3K, we used p110α-myr-MEF and p110β-myr-MEFs. When we normalized CREB3L4 mRNA levels to β-actin levels for MEFs, results were too low to conclude accurate results (Figure 3.7). So we did not continue with analyses on CREB3L4 gene. However, it might be expressed higher in cancerous tissue to see this, further analyses on cancer cell lines like PC3, DU145 might be done. Also, other experimentally validated qPCR primers could have been used as well. Constitutive activation of the PI3K pathway causes an amount of transcript decreased upon pharmacological inhibition of the activated PI3K allele in both SQLE and AK4 gene expressions (Figure 3.7). PI3K activation seems to have a rewiring effect on AK4 and SQLE genes. Also, AK4 did not have catalytic activity, because of its actionable nature, we wanted further analyze the involvement of SQLE in PI3K deregulated human cancers.

In addition to SQLE, we further analyzed other enzymes which are involved in cholesterol synthesis. According to literature, PTEN status difference affects sensitivity to simvastatin which is a HMGCR inhibitor [60]. HMGCR is the first rate-limiting enzyme in cholesterol synthesis pathway. Along these lines, we analyzed first and second rate-limiting enzymes in cholesterol synthesis which are HMGCR, SQLE respectively. This time we searched cholesterol pathway genes in GSE21543 dataset. With constitutive activation of p110β, cholesterol synthesis pathway genes which are HMGCS, MVK, PMVK, FDPS seemed to be upregulated compared to wt prostate tissue except for the MVD gene (Figure 3.8). Then, mRNA levels of cholesterol pathway genes were quantified in PTEN inducible PC3 cells. With PTEN expression, mRNA levels of cholesterol synthesis genes were downregulated (Figure 3.9). So, GSE21543 dataset and our qPCR results show the same phenomenon in alternative experimental approaches, supporting the notion that cholesterol synthesis pathway is

tightly controlled by PI3K. Constitutive PI3K activation leads to increment in cholesterol pathway synthesis genes and PI3K repression by PTEN re-expression cause a reduction in their corresponding mRNA levels. SREBP transcription factor is important for regulation of cholesterol synthesis enzymes and highly amplified in cancerous tissues [28]. Also, we hypothesized that it might be regulated by PI3K pathway leading to wide-spread changes in the expression profiles of genes involved in cholesterol synthesis. It might be further investigated in future studies.

Besides these, cancer biomarker potential of SQLE gene was analyzed with *in silico* datasets. Amplification rate of SQLE gene is high in many cancer types like prostate, breast, ovarian etc. When we look at PTEN mutated samples with SQLE amplification rates, this ratio is highest for breast and prostate cancer patient data. Higher amplification rates in PTEN mutated cancers give some insight into the relation between PTEN and SQLE. Also according to the literature, SQLE overexpression cause epigenetic regulation of PTEN in NAFLD induced hepatocellular carcinoma [76]. Also, many clinical studies were performed in prostate and breast cancer, patients exhibiting lower survival rates with high SQLE expression [77-79]. Overall survival rates of patients with high expression of SQLE were analyzed for prostate and breast cancer patient datasets in cBioPortal. For both cancer types, the overall survival rate was significantly decreased when patients have higher SQLE expression. These results suggest that SQLE could be a potential biomarker to predict progression free survival and potential treatment target for breast and prostate cancer patients.

In the light of the *in silico* and qPCR analyses on SQLE and HMGCR, we wanted to inhibit catalytic activity of genes by using pharmacological inhibitors, namely terbinafine and simvastatin, respectively. Terbinafine and simvastatin are FDA approved drugs [80]. Among the inhibitors which target human SQLE, we moved on with terbinafine because it is more potent inhibitor compared to other SQLE targeting inhibitors like NB-598 and cmpd-4 [81]. Studies claimed that SQLE inhibitors like terbinafine usage lead to regression of prostate tumors with oral drug treatment [82]. These terbinafine screens were also done for ovarian, neuroendocrine cancers and they saw regression of tumor volume [83, 84]. Simvastatin on the other hand, is used as cholesterol lowering agent for cardiovascular diseases, but in this study simvastatin

was used to determine the relationship cholesterol synthesis pathway tumor progression in breast and prostate cancer [85].

Effect of HMGCR and SQLE inhibition on cellular viability with constitutive activation of PI3K was analyzed. Cells that constitutively activated p110β become sensitive to both terbinafine and simvastatin treatment. myr-p110α MEFs became resistant to terbinafine treatment however simvastatin sensitivity did not change compared to wt MEFs. Besides this experiment, we looked at inhibitor treatment effects on breast and prostate cancer cell types that were chosen according to their PTEN-status. Breast and prostate cancer cell types that have wt PTEN were resistant to both terbinafine and simvastatin treatment compared to PTEN-null cell types. So, changes in PI3K activation or PTEN expression cause changes in sensitivity to both inhibitor treatments (Figure 3.13). This situation strengthens the rewiring effect hypothesis between PI3K activation/PTEN status with cholesterol synthesis pathway genes. Effect of PTEN expression on cellular viability of PC3 cells were measured upon PTEN expression induction while 6 days. PC3 cells became resistant to terbinafine treatment but we did not see any difference for simvastatin sensitivity. Induction was done 6 days, so effects might be less pronounced compared to stable expressions.

Biochemical analyses were done to terbinafine and simvastatin treated PTEN-wt DU145 and PTEN-null PC3 cells. In PC3s, we saw a significant reduction in phosphorylation sites which are ser240/244 and ser235/236 of S6 ribosomal protein. P70/p85 S6 kinases regulate phosphorylation of both S235/236 and S240/244 sites but S235/236 phosphorylation occurred by various kinases like protein kinase A (PKA), protein kinase C (PKC) [86]. On the other hand, we did not see any change in p70/p85 S6 kinase levels (Figure 3.15).

4EBP1 can be phosphorylated at many sites by both mTOR and mTOR independent kinases. Ser65 phosphorylation site of 4EBP1 was decreased with terbinafine treatment in PC3 cells. Also, relevant research indicates that Ser65 site might possibly be phosphorylated by GSK3β, ERK and PIM2 [87-89]. Ser65 phosphorylation site is regulated by ERK with leading increased phosphorylation of 4EBP1. Also, phospho-ERK levels were decreased upon both terbinafine and simvastatin treatment in PC3 cells. Maybe decrease in pERK levels lead to less phosphorylation of 4EBP1 which

prevents recruitment of translation initiation complex [90]. PRAS40 phosphorylation at Thr246 was upregulated in both simvastatin and terbinafine treated PC3 cells. However, we could not see any signal for pPRAS40 in DU145 cells. This phosphorylation is known to be promoted by Akt [91].

According to our results, PTEN re-expression also leads to protein degradation of SQLE protein. Also, for protein levels, we saw a decrement in SQLE protein levels with PTEN expression in both PC3 and LNCaP prostate cancer cell lines. HMGCS protein levels were not affected by PTEN expression status even though their mRNA levels were decreased upon PTEN induction (Figure 3.17). Androgen is a steroid and it is important for androgen receptor activity. Androgen receptor is important for prostate tissue development. Hormonal and surgery treatments were commonly applied for prostate cancer patients [92]. However, prostate cancer might recur after hormonal or surgical treatments without depending activity to androgen receptor. Diverse metabolic pathways are activated in androgen independent prostate cancer [93]. However, our inducible PC3 and LNCaP cells show similar outcomes in protein levels of both SQLE and HMGCR. PC3 cells were androgen independent and LNCaP cells were androgen dependent cells [94]. So according to our results in PC3 and LNCaP cells, the dependency on androgen receptor did not cause any difference in terms of protein levels of cholesterol synthesis pathway enzymes.

Our findings on mRNA levels and immunoblots implicate that, PTEN expression status may regulate SQLE gene function. In previous studies, it is suggested that PTEN status is regulated by SQLE gene with epigenetic modifications [76]. However, we wanted to find out whether there is a relation at the translational or post-translational modification level. To find out this process, proteasome inhibitor MG132 was used to inhibit protein degradation. Four hours of MG132 treatment was done for our doxycycline induced and induced PC3s which wt PTEN transfected. Short term proteasome inhibitor treatment was done in order not to induce any changes in gene expression. Normally we saw SQLE protein decrement upon induction, but after MG132 treatment, SQLE were accumulated in PTEN induced PC3s. These results lead to the speculation that PTEN or PI3K activity has a role in post-translational modification of SQLE. Along these lines, it was shown that MARCH6 E3 ubiquitin ligase leads to endoplasmic reticulum related degradation and degradation upon ubiquitylation of SQLE by induction of cholesterol [95]. Also, studies in prostate

cancer showed that Sp1 is the transcriptional regulator of March6 gene. In addition to these, some studies have controversial results on PTEN and SP1 regulation. In some studies, it is reported that PTEN and SP1 negatively regulate each other, but one article claims that PTEN inhibits SP1 phosphorylation [96, 97]. These dependencies might be further researched and controversial findings need to be clarified.

Increased amount of lipid metabolites were observed in brain metastatic cells. However, mouse brain tissue has lower levels of triacylglycerols. The abundance of cholesterol, membrane lipids and triacylglycerols were indicated as a signature associated with metastasis of breast cancer to the brain. [98]. Lipid metabolism signature enrichment like SREBF1 and stearoyl-CoA desaturase was unique to only brain metastasis, not other tissue metastases. These insights further demonstrate the effect of lipid metabolism on metastasis. [98]. For tamoxifen therapy retrieved patient database analyses on Roc PLotter, only SQLE gene has significant change between responders and nonresponders to tamoxifen treatment. Besides breast cancer patients that did not respond to tamoxifen therapy, have higher SQLE expression and lower progression free survival rate. SQLE levels were increased in tamoxifen resistant breast cancer line in our study. Other cholesterol pathway synthesis gene enzymes did not cause significant changes for relapse-free survival. Also, PIK3CA mutations were correlated with brain metastasis of breast cancer [98] and we used T47D cells to see affects of tamoxifen *in vitro*. Tamoxifen resistant T47D which is a PI3CA mutated breast cancer cell line was produced upon long term treatment of progressively increasing doses of tamoxifen. Tamoxifen treatment in the long run causes PI3K pathway upregulation. SQLE protein level was upregulated in tamoxifen resistant T47D cells compared to parental T47Ds and HMGCS levels were not changed. SQLE protein upregulation and lower survival rates of patients strengthen the biomarker potential of SQLE.

When we looked at the cholesterol synthesis inhibitors, statin usage had shown to have some effect on tumor regression with prostate and breast cancer studies [99, 100]. However, statins cause many side effects like impaired insulin secretion, impaired mitochondrial function [101]. Since statins cause decrement in production of metabolites which are highly important in cellular physiology e.g. geranyl-geranyl pyro-phosphate, mevalonate. If SQLE inhibitors are used for cancer treatment instead

of statins, cholesterol pathway will be targeted at later stages and it might prevent chemotoxic effects of statins to a certain extent.

In addition to these, drug repurposing is an intriguing alternative for disease treatment instead of drug synthesizing *de novo*. It is highly encouraged way to use new drugs for cancer treatments or other diseases [102]. Because of these reasons usage of terbinafine might be beneficial to patients for combinational therapies. However, the efficiency of SQLE inhibitors might be improved because higher concentrations of drugs were used for effective regression in proliferation. All in all, PI3K pathway activation has an impact on cholesterol pathway synthesis enzymes. One of the rate-limiting enzymes of cholesterol synthesis, SQLE seem to have potential to be a candidate biomarker gene for PTEN-null and tamoxifen resistant cancers.

Chapter 5

Conclusion and Future Perspectives

In our study, I investigated ClassIA isoform of PI3K dependence change in PTEN-loss driven cancer models. Firstly, the effect of PTEN was investigated in mesenchymal, untransformed MEFs and metastatic prostate cancer cell line PC3. With these experiments, we investigated PTEN-PI3K isoform dependence in complementary approaches. We found out that PTEN expression change affects the predominance level of PI3K isoform. Also, p110β overexpression on top of PTEN depletion, cause both regression of p110α predominance and higher dependence to p110β isoform in MEFs.

Then metabolic regulations were investigated upon constitutively activated p110β in prostate tissue of mice. AK4, CREB3L4 and SQLE mRNA levels were found to be significantly upregulated upon constitutive activation of PI3K in early lesions of prostate cancer. I think AK4 and CREB3L4 genes were also promising candidate genes in relation to PI3K isoform dependence change. Further investigations could be performed to characterize their putative roles in regulating PI3K induced metabolic events. In addition to these, functional interaction of SQLE and PTEN might be further investigated. Potential post-translational modifications of SQLE e.g. phosphorylation, acetylation, sumoylation might be further characterized.

According to my *in silico* analyses, SQLE has high potential for being biomarker for prostate and breast cancer as well as PTEN-null cancers. Also, mRNA levels of cholesterol synthesis pathway genes were decreased upon PTEN induction, implicating a more general mode of regulation. SREBP transcription factor is known to be master regulator of cholesterol synthesis pathway [28] and it might be a potential follow up research for cholesterol synthesis and PTEN relation.

Pharmacological inhibition of cholesterol synthesis pathway with simvastatin and terbinafine, caused sensitivity in inherently PTEN-null breast and prostate cell lines compared to PTEN-wt cell lines. PTEN-null PC3 had lower PI3K downstream pathway activation upon inhibitor treatments compared to PTEN-wt DU145 cells. Also, constitutive activation of p110β in MEFs caused higher sensitivity for both cholesterol synthesis pathway rate limiting enzyme inhibitions. Both mRNA and

protein levels of SQLE is changed upon PTEN induction. Upon short-term proteasome inhibitor treatment, SQLE accumulation occurred which indicated the post-translational impact of PTEN on SQLE. According to literature, March6 is responsible for SQLE degradation and March6 or other proteins that are involved in SQLE stability can be investigated in respect to PTEN.

All in all, pan-PI3K inhibitors or p110β monotherapies to PTEN-null tumors were not efficient and they caused transient effect on tumor regression. However combinational therapies were investigated for alternative therapies for PTEN-null cancers. According to our study, SQLE and cholesterol synthesis pathway relation with PTEN might be an intriguing way for combinational treatments. Also, with drug repurposing of terbinafine which is FDA approved drug fungal infections usage in tumor regression. Its effects might be further investigated with in vivo studies and terbinafine could be a possible treatment option for PTEN-null cancers if its human SQLE gene targeting efficiency of terbinafine improved. In addition to these, development of more specific and potent SQLE inhibitors might be a therapeutic option in the longer run.

Bibliography

1. Cantley, L.C., *The phosphoinositide 3-kinase pathway.* Science, 2002. **296**(5573): p. 1655-7.
2. Liu, P., et al., *Targeting the phosphoinositide 3-kinase pathway in cancer.* Nat Rev Drug Discov, 2009. **8**(8): p. 627-44.
3. Vanhaesebroeck, B., et al., *Synthesis and function of 3-phosphorylated inositol lipids.* Annu Rev Biochem, 2001. **70**: p. 535-602.
4. Vanhaesebroeck, B., et al., *The emerging mechanisms of isoform-specific PI3K signalling.* Nat Rev Mol Cell Biol, 2010. **11**(5): p. 329-41.
5. Hiles, I.D., et al., *Phosphatidylinositol 3-kinase: structure and expression of the 110 kd catalytic subunit.* Cell, 1992. **70**(3): p. 419-29.
6. Inukai, K., et al., *Five isoforms of the phosphatidylinositol 3-kinase regulatory subunit exhibit different associations with receptor tyrosine kinases and their tyrosine phosphorylations.* FEBS Lett, 2001. **490**(1-2): p. 32-8.
7. Chantry, D., et al., *p110delta, a novel phosphatidylinositol 3-kinase catalytic subunit that associates with p85 and is expressed predominantly in leukocytes.* J Biol Chem, 1997. **272**(31): p. 19236-41.
8. Fritsch, R., et al., *RAS and RHO families of GTPases directly regulate distinct phosphoinositide 3-kinase isoforms.* Cell, 2013. **153**(5): p. 1050-63.
9. Dbouk, H.A., *PI3King the right partner: unique interactions and signaling by p110β.* Postdoc J, 2015. **3**(6): p. 71-87.
10. Alessi, D.R., et al., *Characterization of a 3-phosphoinositide-dependent protein kinase which phosphorylates and activates protein kinase Balpha.* Curr Biol, 1997. **7**(4): p. 261-9.
11. Bruhn, M.A., et al., *AKT-independent PI3-K signaling in cancer - emerging role for SGK3.* Cancer Manag Res, 2013. **5**: p. 281-92.
12. Malik, N., et al., *Mechanism of activation of SGK3 by growth factors via the Class 1 and Class 3 PI3Ks.* Biochem J, 2018. **475**(1): p. 117-135.
13. Alimonti, A., et al., *Subtle variations in Pten dose determine cancer susceptibility.* Nat Genet, 2010. **42**(5): p. 454-8.
14. Suzuki, A., et al., *High cancer susceptibility and embryonic lethality associated with mutation of the PTEN tumor suppressor gene in mice.* Curr Biol, 1998. **8**(21): p. 1169-78.
15. Bubien, V., et al., *High cumulative risks of cancer in patients with PTEN hamartoma tumour syndrome.* J Med Genet, 2013. **50**(4): p. 255-63.
16. Stambolic, V., et al., *Negative regulation of PKB/Akt-dependent cell survival by the tumor suppressor PTEN.* Cell, 1998. **95**(1): p. 29-39.
17. Wang, X. and X. Jiang, *PTEN: a default gate-keeping tumor suppressor with a versatile tail.* Cell Res, 2008. **18**(8): p. 807-16.
18. Myers, M.P., et al., *P-TEN, the tumor suppressor from human chromosome 10q23, is a dual-specificity phosphatase.* Proc Natl Acad Sci U S A, 1997. **94**(17): p. 9052-7.
19. Zack, T.I., et al., *Pan-cancer patterns of somatic copy number alteration.* Nat Genet, 2013. **45**(10): p. 1134-40.
20. Zhang, Y., et al., *A Pan-Cancer Proteogenomic Atlas of PI3K/AKT/mTOR Pathway Alterations.* Cancer Cell, 2017. **31**(6): p. 820-832 e3.
21. Sanchez-Vega, F., et al., *Oncogenic Signaling Pathways in The Cancer Genome Atlas.* Cell, 2018. **173**(2): p. 321-337 e10.
22. Millis, S.Z., et al., *Landscape of Phosphatidylinositol-3-Kinase Pathway Alterations Across 19784 Diverse Solid Tumors.* JAMA Oncol, 2016. **2**(12): p. 1565-1573.

23. Manning, B.D. and A. Toker, *AKT/PKB Signaling: Navigating the Network.* Cell, 2017. **169**(3): p. 381-405.
24. Valvezan, A.J. and B.D. Manning, *Molecular logic of mTORC1 signalling as a metabolic rheostat.* Nature Metabolism, 2019. **1**(3): p. 321-333.
25. Moores, S.L., et al., *Sequence dependence of protein isoprenylation.* J Biol Chem, 1991. **266**(22): p. 14603-10.
26. Lobell, R.B., *Prenylation of Ras GTPase superfamily proteins and their function in immunobiology.* Adv Immunol, 1998. **68**: p. 145-89.
27. Huang, B., B.-l. Song, and C. Xu, *Cholesterol metabolism in cancer: mechanisms and therapeutic opportunities.* Nature Metabolism, 2020. **2**(2): p. 132-141.
28. Lewis, C.A., et al., *SREBP maintains lipid biosynthesis and viability of cancer cells under lipid- and oxygen-deprived conditions and defines a gene signature associated with poor survival in glioblastoma multiforme.* Oncogene, 2015. **34**(40): p. 5128-40.
29. Lee, B.H., et al., *Dysregulation of cholesterol homeostasis in human prostate cancer through loss of ABCA1.* Cancer Res, 2013. **73**(3): p. 1211-8.
30. Stopsack, K.H., et al., *Cholesterol uptake and regulation in high-grade and lethal prostate cancers.* Carcinogenesis, 2017. **38**(8): p. 806-811.
31. Yue, S., et al., *Cholesteryl ester accumulation induced by PTEN loss and PI3K/AKT activation underlies human prostate cancer aggressiveness.* Cell Metab, 2014. **19**(3): p. 393-406.
32. Marcelli, M., et al., *Androgen receptor mutations in prostate cancer.* Cancer Res, 2000. **60**(4): p. 944-9.
33. Yeh, S., et al., *From HER2/Neu signal cascade to androgen receptor and its coactivators: a novel pathway by induction of androgen target genes through MAP kinase in prostate cancer cells.* Proc Natl Acad Sci U S A, 1999. **96**(10): p. 5458-63.
34. Attard, G., C.S. Cooper, and J.S. de Bono, *Steroid hormone receptors in prostate cancer: a hard habit to break?* Cancer Cell, 2009. **16**(6): p. 458-62.
35. Jiao, J., et al., *Murine cell lines derived from Pten null prostate cancer show the critical role of PTEN in hormone refractory prostate cancer development.* Cancer Res, 2007. **67**(13): p. 6083-91.
36. Carver, B.S., et al., *Reciprocal feedback regulation of PI3K and androgen receptor signaling in PTEN-deficient prostate cancer.* Cancer Cell, 2011. **19**(5): p. 575-86.
37. Mulholland, D.J., et al., *Cell autonomous role of PTEN in regulating castration-resistant prostate cancer growth.* Cancer Cell, 2011. **19**(6): p. 792-804.
38. Raval, A.D., et al., *Association between statins and clinical outcomes among men with prostate cancer: a systematic review and meta-analysis.* Prostate Cancer and Prostatic Diseases, 2016. **19**(2): p. 151-162.
39. Islam, M., et al., *Atorvastatin inhibits RhoC function and limits head and neck cancer metastasis.* Oral Oncol, 2013. **49**(8): p. 778-86.
40. Campbell, M.J., et al., *Breast cancer growth prevention by statins.* Cancer Res, 2006. **66**(17): p. 8707-14.
41. Lee, S.H., et al., *A constitutively activated form of the p110β isoform of PI3-kinase induces prostatic intraepithelial neoplasia in mice.* Proceedings of the National Academy of Sciences, 2010. **107**(24): p. 11002-11007.
42. Cerami, E., et al., *The cBio Cancer Genomics Portal: An Open Platform for Exploring Multidimensional Cancer Genomics Data.* Cancer Discovery, 2012. **2**(5): p. 401-404.
43. Thorpe, L.M., H. Yuzugullu, and J.J. Zhao, *PI3K in cancer: divergent roles of isoforms, modes of activation and therapeutic targeting.* Nature Reviews Cancer, 2015. **15**(1): p. 7-24.

44. Zhao, J.J., et al., *The p110alpha isoform of PI3K is essential for proper growth factor signaling and oncogenic transformation.* Proc Natl Acad Sci U S A, 2006. **103**(44): p. 16296-300.
45. Wee, S., et al., *PTEN-deficient cancers depend on PIK3CB.* Proc Natl Acad Sci U S A, 2008. **105**(35): p. 13057-62.
46. Ni, J., et al., *Functional characterization of an isoform-selective inhibitor of PI3K-p110β as a potential anticancer agent.* Cancer Discov, 2012. **2**(5): p. 425-33.
47. Kang, S., et al., *Oncogenic transformation induced by the p110β, -γ, and -δ isoforms of class I phosphoinositide 3-kinase.* Proceedings of the National Academy of Sciences, 2006. **103**(5): p. 1289-1294.
48. Folkes, A.J., et al., *The identification of 2-(1H-indazol-4-yl)-6-(4-methanesulfonyl-piperazin-1-ylmethyl)-4-morpholin-4-yl-thieno[3,2-d]pyrimidine (GDC-0941) as a potent, selective, orally bioavailable inhibitor of class I PI3 kinase for the treatment of cancer.* J Med Chem, 2008. **51**(18): p. 5522-32.
49. Ciraolo, E., et al., *Phosphoinositide 3-kinase p110beta activity: key role in metabolism and mammary gland cancer but not development.* Sci Signal, 2008. **1**(36): p. ra3.
50. Jia, S., et al., *Essential roles of PI(3)K-p110beta in cell growth, metabolism and tumorigenesis.* Nature, 2008. **454**(7205): p. 776-9.
51. Xiao, H., et al., *Inhibition of Rho and Rac geranylgeranylation by atorvastatin is critical for preservation of endothelial junction integrity.* PLoS One, 2013. **8**(3): p. e59233.
52. Barrett, T., et al., *NCBI GEO: archive for functional genomics data sets—update.* Nucleic Acids Research, 2012. **41**(D1): p. D991-D995.
53. Huang da, W., B.T. Sherman, and R.A. Lempicki, *Systematic and integrative analysis of large gene lists using DAVID bioinformatics resources.* Nat Protoc, 2009. **4**(1): p. 44-57.
54. Sui, Z., et al., *Squalene epoxidase (SQLE) promotes the growth and migration of the hepatocellular carcinoma cells.* Tumour Biol, 2015. **36**(8): p. 6173-9.
55. Ge, H., et al., *Squalene epoxidase promotes the proliferation and metastasis of lung squamous cell carcinoma cells though extracellular signal-regulated kinase signaling.* Thorac Cancer, 2019. **10**(3): p. 428-436.
56. Zhang, J., et al., *AK4 Promotes the Progression of HER2-Positive Breast Cancer by Facilitating Cell Proliferation and Invasion.* Disease Markers, 2019. **2019**: p. 8186091.
57. Kim, T.H., et al., *The role of CREB3L4 in the proliferation of prostate cancer cells.* Sci Rep, 2017. **7**: p. 45300.
58. Pu, Q., et al., *The Novel Transcription Factor CREB3L4 Contributes to the Progression of Human Breast Carcinoma.* J Mammary Gland Biol Neoplasia, 2020. **25**(1): p. 37-50.
59. Liu, R., et al., *Enzymatically inactive adenylate kinase 4 interacts with mitochondrial ADP/ATP translocase.* Int J Biochem Cell Biol, 2009. **41**(6): p. 1371-80.
60. Cizmecioglu, O., et al., *Rac1-mediated membrane raft localization of PI3K/p110β is required for its activation by GPCRs or PTEN loss.* Elife, 2016. **5**.
61. Albertson, D.G., *Gene amplification in cancer.* Trends Genet, 2006. **22**(8): p. 447-55.
62. Torti, D. and L. Trusolino, *Oncogene addiction as a foundational rationale for targeted anti-cancer therapy: promises and perils.* EMBO Mol Med, 2011. **3**(11): p. 623-36.
63. Ding, X., et al., *The role of cholesterol metabolism in cancer.* Am J Cancer Res, 2019. **9**(2): p. 219-227.
64. Buhaescu, I. and H. Izzedine, *Mevalonate pathway: a review of clinical and therapeutical implications.* Clin Biochem, 2007. **40**(9-10): p. 575-84.

65. Zhou, X., et al., *Effect of PTEN loss on metabolic reprogramming in prostate cancer cells.* Oncol Lett, 2019. **17**(3): p. 2856-2866.
66. DeBose-Boyd, R.A., *Feedback regulation of cholesterol synthesis: sterol-accelerated ubiquitination and degradation of HMG CoA reductase.* Cell Res, 2008. **18**(6): p. 609-21.
67. Fekete, J.T. and B. Győrffy, *ROCplot.org: Validating predictive biomarkers of chemotherapy/hormonal therapy/anti-HER2 therapy using transcriptomic data of 3,104 breast cancer patients.* Int J Cancer, 2019. **145**(11): p. 3140-3151.
68. Mishra, R.R., et al., *Reactivation of cAMP Pathway by PDE4D Inhibition Represents a Novel Druggable Axis for Overcoming Tamoxifen Resistance in ER-positive Breast Cancer.* Clinical Cancer Research, 2018. **24**(8): p. 1987-2001.
69. Sweeney, E.E., et al., *Models and Mechanisms of Acquired Antihormone Resistance in Breast Cancer: Significant Clinical Progress Despite Limitations.* Horm Mol Biol Clin Investig, 2012. **9**(2): p. 143-163.
70. Bauer, T.M., M.R. Patel, and J.R. Infante, *Targeting PI3 kinase in cancer.* Pharmacol Ther, 2015. **146**: p. 53-60.
71. Hancox, U., et al., *Inhibition of PI3Kβ signaling with AZD8186 inhibits growth of PTEN-deficient breast and prostate tumors alone and in combination with docetaxel.* Mol Cancer Ther, 2015. **14**(1): p. 48-58.
72. Sethi, I., et al., *Molecular Profiling Establishes Genetic Features Predictive of the Efficacy of the p110β Inhibitor KIN-193.* Cancer Res, 2019. **79**(17): p. 4524-4531.
73. Costa, C., et al., *Measurement of PIP3 levels reveals an unexpected role for p110β in early adaptive responses to p110α-specific inhibitors in luminal breast cancer.* Cancer Cell, 2015. **27**(1): p. 97-108.
74. Schwartz, S., et al., *Feedback suppression of PI3Kα signaling in PTEN-mutated tumors is relieved by selective inhibition of PI3Kβ.* Cancer Cell, 2015. **27**(1): p. 109-22.
75. Certal, V., et al., *Discovery and Optimization of Pyrimidone Indoline Amide PI3Kβ Inhibitors for the Treatment of Phosphatase and Tensin Homologue (PTEN)-Deficient Cancers.* Journal of Medicinal Chemistry, 2014. **57**(3): p. 903-920.
76. Liu, D., et al., *Squalene epoxidase drives NAFLD-induced hepatocellular carcinoma and is a pharmaceutical target.* Sci Transl Med, 2018. **10**(437).
77. Stopsack, K.H., et al., *Cholesterol Metabolism and Prostate Cancer Lethality.* Cancer Res, 2016. **76**(16): p. 4785-90.
78. Stopsack, K.H., et al., *Cholesterol uptake and regulation in high-grade and lethal prostate cancers.* Carcinogenesis, 2017. **38**(8): p. 806-811.
79. Brown, D.N., et al., *Squalene epoxidase is a bona fide oncogene by amplification with clinical relevance in breast cancer.* Sci Rep, 2016. **6**: p. 19435.
80. Petranyi, G., N.S. Ryder, and A. Stütz, *Allylamine derivatives: new class of synthetic antifungal agents inhibiting fungal squalene epoxidase.* Science, 1984. **224**(4654): p. 1239-41.
81. Padyana, A.K., et al., *Structure and inhibition mechanism of the catalytic domain of human squalene epoxidase.* Nat Commun, 2019. **10**(1): p. 97.
82. Ji, J., J. Sundquist, and K. Sundquist, *Use of terbinafine and risk of death in patients with prostate cancer: A population-based cohort study.* Int J Cancer, 2019. **144**(8): p. 1888-1895.
83. Motamedian, E., E. Taheri, and F. Bagheri, *Proliferation inhibition of cisplatin-resistant ovarian cancer cells using drugs screened by integrating a metabolic model and transcriptomic data.* Cell Prolif, 2017. **50**(6).
84. Mahoney, C.E., et al., *A chemical biology screen identifies a vulnerability of neuroendocrine cancer cells to SQLE inhibition.* Nat Commun, 2019. **10**(1): p. 96.

85. Ahern, T.P., et al., *Statins and breast cancer prognosis: evidence and opportunities.* Lancet Oncol, 2014. **15**(10): p. e461-8.
86. Biever, A., E. Valjent, and E. Puighermanal, *Ribosomal Protein S6 Phosphorylation in the Nervous System: From Regulation to Function.* Frontiers in Molecular Neuroscience, 2015. **8**(75).
87. Shin, S., et al., *Glycogen synthase kinase-3β positively regulates protein synthesis and cell proliferation through the regulation of translation initiation factor 4E-binding protein 1.* Oncogene, 2014. **33**(13): p. 1690-9.
88. Haystead, T.A., et al., *Phosphorylation of PHAS-I by mitogen-activated protein (MAP) kinase. Identification of a site phosphorylated by MAP kinase in vitro and in response to insulin in rat adipocytes.* J Biol Chem, 1994. **269**(37): p. 23185-91.
89. Fox, C.J., et al., *The serine/threonine kinase Pim-2 is a transcriptionally regulated apoptotic inhibitor.* Genes Dev, 2003. **17**(15): p. 1841-54.
90. Qin, X., B. Jiang, and Y. Zhang, *4E-BP1, a multifactor regulated multifunctional protein.* Cell Cycle, 2016. **15**(6): p. 781-6.
91. Nascimento, E.B., et al., *Phosphorylation of PRAS40 on Thr246 by PKB/AKT facilitates efficient phosphorylation of Ser183 by mTORC1.* Cell Signal, 2010. **22**(6): p. 961-7.
92. Abd Wahab, N.A., et al., *Mechanism of Anti-Cancer Activity of Curcumin on Androgen-Dependent and Androgen-Independent Prostate Cancer.* Nutrients, 2020. **12**(3).
93. Ferraldeschi, R., et al., *Targeting the androgen receptor pathway in castration-resistant prostate cancer: progresses and prospects.* Oncogene, 2015. **34**(14): p. 1745-1757.
94. Saraon, P., et al., *Proteomic profiling of androgen-independent prostate cancer cell lines reveals a role for protein S during the development of high grade and castration-resistant prostate cancer.* J Biol Chem, 2012. **287**(41): p. 34019-31.
95. Tan, J.M.E., et al., *The MARCH6-SQLE Axis Controls Endothelial Cholesterol Homeostasis and Angiogenic Sprouting.* Cell Rep, 2020. **32**(5): p. 107944.
96. Kou, X.-X., et al., *Acetylated Sp1 inhibits PTEN expression through binding to PTEN core promoter and recruitment of HDAC1 and promotes cancer cell migration and invasion.* Carcinogenesis, 2012. **34**(1): p. 58-67.
97. Kang-Park, S., Y.I. Lee, and Y.I. Lee, *PTEN modulates insulin-like growth factor II (IGF-II)-mediated signaling; the protein phosphatase activity of PTEN downregulates IGF-II expression in hepatoma cells.* FEBS Lett, 2003. **545**(2-3): p. 203-8.
98. Jin, X., et al., *A metastasis map of human cancer cell lines.* Nature, 2020. **588**(7837): p. 331-336.
99. Beckwitt, C.H., et al., *Statin drugs to reduce breast cancer recurrence and mortality.* Breast Cancer Res, 2018. **20**(1): p. 144.
100. Pernar, C.H., et al., *The Epidemiology of Prostate Cancer.* Cold Spring Harb Perspect Med, 2018. **8**(12).
101. Thompson, P.D., et al., *Statin-Associated Side Effects.* J Am Coll Cardiol, 2016. **67**(20): p. 2395-2410.
102. Bertolini, F., V.P. Sukhatme, and G. Bouche, *Drug repurposing in oncology--patient and health systems opportunities.* Nat Rev Clin Oncol, 2015. **12**(12): p. 732-42.

Appendix

Copyright permissions

SPRINGER NATURE LICENSE
TERMS AND CONDITIONS

Oct 01, 2020

This Agreement between Ms. Sena Atıcı ("You") and Springer Nature ("Springer Nature") consists of your license details and the terms and conditions provided by Springer Nature and Copyright Clearance Center.

License Number	4920450011608
License date	Oct 01, 2020
Licensed Content Publisher	Springer Nature
Licensed Content Publication	Nature Reviews Drug Discovery
Licensed Content Title	Targeting the phosphoinositide 3-kinase pathway in cancer
Licensed Content Author	Pixu Liu et al
Licensed Content Date	Dec 31, 1969
Type of Use	Thesis/Dissertation
Requestor type	academic/university or research institute
Format	print and electronic
Portion	figures/tables/illustrations
Number of figures/tables/illustrations	1
Will you be translating?	no
Circulation/distribution	1 - 29

Author of this Springer Nature content	no
Title	Molecular Mechanisms of PI3K Isoform Dependence in Carcinogenesis
Institution name	Bilkent University
Expected presentation date	Oct 2020
Portions	Figure 1
Requestor Location	Ms. Sena Atıcı ÜNiversiteler Mah Merkez Kampüs Ankara, 06800 Turkey Attn: Ms. Sena Atıcı
Total	0.00 USD

SPRINGER NATURE LICENSE
TERMS AND CONDITIONS

Nov 25, 2020

This Agreement between Ms. Sena Atıcı ("You") and Springer Nature ("Springer Nature") consists of your license details and the terms and conditions provided by Springer Nature and Copyright Clearance Center.

License Number	4956110915453
License date	Nov 25, 2020
Licensed Content Publisher	Springer Nature
Licensed Content Publication	Nature Reviews Molecular Cell Biology
Licensed Content Title	The emerging mechanisms of isoform-specific PI3K signalling
Licensed Content Author	Bart Vanhaesebroeck et al
Licensed Content Date	Apr 9, 2010
Type of Use	Thesis/Dissertation
Requestor type	academic/university or research institute
Format	print and electronic
Portion	figures/tables/illustrations
Number of figures/tables/illustrations	2
High-res required	no
Will you be translating?	no
Circulation/distribution	1 - 29
Author of this Springer Nature content	no
Title	Molecular Mechanisms of PI3K Isoform Dependence in Carcinogenesis
Institution name	Bilkent University
Expected presentation date	Dec 2020
Portions	Figure 2
Requestor Location	Ms. Sena Atıcı ÜNiversiteler Mah Merkez Kampüs Ankara, 06800 Turkey Attn: Ms. Sena Atıcı
Total	0.00 USD

SPRINGER NATURE LICENSE
TERMS AND CONDITIONS

Nov 25, 2020

This Agreement between Ms. Sena Atıcı ("You") and Springer Nature ("Springer Nature") consists of your license details and the terms and conditions provided by Springer Nature and Copyright Clearance Center.

License Number	4956111400481
License date	Nov 25, 2020
Licensed Content Publisher	Springer Nature
Licensed Content Publication	Cell Research
Licensed Content Title	PTEN: a default gate-keeping tumor suppressor with a versatile tail
Licensed Content Author	Xinjiang Wang et al
Licensed Content Date	Jul 15, 2008
Type of Use	Thesis/Dissertation
Requestor type	academic/university or research institute
Format	print and electronic
Portion	figures/tables/illustrations
Number of figures/tables/illustrations	1
High-res required	no
Will you be translating?	no
Circulation/distribution	1 - 29
Author of this Springer Nature content	no
Title	Molecular Mechanisms of PI3K Isoform Dependence in Carcinogenesis
Institution name	Bilkent University
Expected presentation date	Dec 2020
Portions	Figure 1
Requestor Location	Ms. Sena Atıcı ÜNiversiteler Mah Merkez Kampüs Ankara, 06800 Turkey Attn: Ms. Sena Atıcı
Total	0.00 USD

SPRINGER NATURE LICENSE
TERMS AND CONDITIONS

Nov 25, 2020

This Agreement between Ms. Sena Atıcı ("You") and Springer Nature ("Springer Nature") consists of your license details and the terms and conditions provided by Springer Nature and Copyright Clearance Center.

License Number	4956120459436
License date	Nov 25, 2020
Licensed Content Publisher	Springer Nature
Licensed Content Publication	Nature Metabolism
Licensed Content Title	Cholesterol metabolism in cancer: mechanisms and therapeutic opportunities
Licensed Content Author	Binlu Huang et al
Licensed Content Date	Feb 10, 2020
Type of Use	Thesis/Dissertation
Requestor type	academic/university or research institute
Format	print and electronic
Portion	figures/tables/illustrations
Number of figures/tables/illustrations	1
Will you be translating?	no
Circulation/distribution	1 - 29
Author of this Springer Nature content	no
Title	Molecular Mechanisms of PI3K Isoform Dependence in Carcinogenesis
Institution name	Bilkent University
Expected presentation date	Dec 2020
Portions	Figure 1
Requestor Location	Ms. Sena Atıcı ÜNiversiteler Mah Merkez Kampüs Ankara, 06800 Turkey Attn: Ms. Sena Atıcı
Total	0.00 USD